CBI			
CI/SfB			
Date: April 1997			

THE RESOURCE CENTRE FOR BUILDING EXCELLENCE

STUDY REPORT

No 77 (1997)

Sheathing Contributions to Wall Element Strength and Stiffness

B.L. Deam
G.J. Beattie

RESTRICTED

The work reported here was funded by the Foundation for Research, Science and Technology from the Public Good Science Fund, and by the Building Research Levy.

ISSN: 0113-3675

PREFACE

This study forms the first phase of an investigation to quantify the degree of interaction between timber structural framing components and non-structural sheathings and their effect on the stiffness and strength of the structural framing when subjected to axial loadings and out-of-plane face loadings.

ACKNOWLEDGEMENTS

The authors acknowledge the financial support for this study from the Building Research Levy and the Public Good Science Fund of the Foundation for Research, Science and Technology. The assistance of Winstone Wallboards Ltd and James Hardie Building Products Ltd is also acknowledged.

READERSHIP

This report is intended for researchers and engineers.

Sheathing Contributions to Wall Element Strength and Stiffness

BRANZ Study Report SR 77

B.L.Deam
G.J.Beattie

Reference

Deam, B.L. and Beattie, G.J. 1997. Sheathing Contributions to Wall Element Strength and Stiffness. Building Research Association of New Zealand. Study Report SR 77 , Judgeford.

KEYWORDS

Timber framing; Composite action; Sheathings; Wind loads.

ABSTRACT

It is commonly known that a degree of interaction exists between the timber framing members and non-structural components and sheathings of timber structures. Some prescriptive codes contain implicit assumptions about this interaction, but the actual degree of composite behaviour is not always clear.

This project investigated the stiffness enhancement of studs sheathed with internal and external sheet materials when subjected to simultaneously applied axial and face loading, the strength of connections typically used between top framing plates and truss or rafter members under uplift loading and the top plate stiffness enhancement provided by internal and external sheet materials.

Results indicated that the out-of-plane bending stiffness enhancement offered to studs by gypsum plasterboard and fibre-cement sheet sheathings was at least 60% for gypsum plasterboard only on one side and at least 150% for gypsum plasterboard on one side and fibre-cement sheet on the other. The strengths of the connections, between the studs and top plate and between the top plate and trusses or rafters currently specified by the New Zealand non-specific design code for timber frame buildings were found to be less than the expected uplift loads calculated by the New Zealand loadings code. Wall sheathings were shown to have a beneficial influence on the weak axis bending load-resisting capability of top plates. However, an analytical model which takes account of the modulus of elasticity of the top plate and the strength and stiffness parameters for the sheathing fasteners gave an underestimate of the deflection behaviour of the system.

1. Introduction

The Code of Practice for Light Timber Frame Buildings Not Requiring Specific Design, NZS 3604 (SNZ,1990) contains implicit assumptions that a degree of interaction exists between the timber framing members and non-structural components such as sheathings. For example, sheathings are assumed to provide stability to studs against buckling about their weak axis through their connections. Hence, the structural timber dimensions are often reduced below those that would be required if they were designed using the Timber Structures Standard, NZS 3603 (SNZ,1993), on which NZS 3604 is based. NZS 3603 and the loadings standard, NZS 4203 (SNZ,1992), have recently been changed from working stress design principles to limit state design principles in an effort to make the reasoning behind these standards more transparent to the user.

Non-structural components such as sheathings can be shown to contribute to both the strength and stiffness of timber framed construction systems. This occurs through a combination of composite action where the sheathings act as flange members to the framing, and load sharing where the transverse stiffness of the sheathing draws adjacent framing members into action. Complete composite action occurs when the sheathing and structural member act as one. However, this effect reduces because of slip in the fasteners which attach the sheathing to the structural member. Load sharing occurs when the sheathing redistributes load from a relatively flexible member to adjacent stiffer members.

Stud walls cannot realistically be modelled as simple beam-column systems because these do not account for load sharing or composite action. Most research into the behaviour of light timber frame walls was carried out at Oregon State University and the Forest Products Laboratory during the '70s and '80s (Polensek [1976], Polensek and Atherton [1976], Polensek and Schimel [1986] and Sherwood and Moody [1989]).

Only a limited amount of US research has focused on modelling the behaviour of wall elements subjected to either face loading or combined face and axial loading (Gromala and Polensek [1984]). A series of research projects, summarised by Deam and King (1994) for the Australian National Association of Forest Industries (NAFI), developed design procedures for walls, floors, rafters, lintels and top plates. This work extends the models developed for the NAFI research projects and calibrates them for the loads and building details typically encountered in New Zealand buildings.

The study which follows was conducted as three separate investigations. The first investigated the stiffness enhancement of studs sheathed with internal and external sheet materials when subjected to simultaneously applied axial and face loading. The second investigated the strength of connections typically used between top framing plates and truss or rafter members under uplift loading. The third investigated the top plate stiffness enhancement provided by internal and external sheet materials.

Each investigation had a literature review phase, an analytical phase, an experimental phase and a summary phase where the results of the analytical and experimental phases were compared. All phases of each investigation are grouped together in the report. Because composite action was not a contributor to the behaviour of the rafter/top plate/stud connections, there was no analytical phase in that investigation.

2. Composite Action of Wall Studs and Claddings

2.1 Literature Review

Polensek (1976) developed a finite element computer program, FINWALL, to predict the deflections, stresses and ultimate loads of light timber stud walls subjected to both axial and face loads. Four I-beam elements were used to model each stud, with composite action from sheathing nailed to one or both faces. The series of solutions for stressed skin panels published by Amana and Booth (1967) was used to determine the degree of composite action. Load sharing between the studs was modelled with plate elements between the I-beam elements. Eccentric axial load on the studs was replaced with out-of-plane loads at three points on the face by an iterative method, to reduce the size of the stiffness matrix in the computer model. The model accurately predicted the behaviour of a 2.4m high by 3.6m wide wall with five Douglas fir studs and faces sheathed with plywood and gypsum plasterboard respectively. The model was calibrated by removing the unbroken studs, with the sheathing still attached, and measuring the deflection with a simple bending test. These values were then used in FINWALL to predict the behaviour of the wall with different stud sequences. Results of the five stud wall tests were published separately (Polensek and Atherton, 1976).

FINWALL was able to accurately model the composite action between the studs and wall linings as well as the load sharing between studs. Wall stiffness was initially shown to be highly dependent upon the moduli of elasticity of the studs and wall linings and the slip moduli of the nail connections. Later studies by Gromala and Polensek (1984) indicated that wall behaviour was less sensitive to the sheathing elastic modulus and concluded that research should focus upon the stud modulus of elasticity and the sheathing fastener load-slip characteristics.

FINWALL was also used for probabilistic analysis of wall strength by analysing walls designed with timber randomly selected from a large number of laboratory tested Douglas fir and Southern pine samples (Gromala and Polensek, 1983).

The stud end conditions were then identified as significantly influencing the behaviour of the wall. Polensek and Schimel (1986) modelled a typical wall to floor and foundation connection with non-linear finite elements. These had Douglas fir studs, an internal sheathing of 10 mm thick gypsum plasterboard and an exterior sheathing of plywood, hardboard or fibreboard. The external sheathing was attached to the sill plate beneath the joists rather than to the bottom wall plate. Out-of-plane deflections predicted by the model agreed closely with the measured deflections of nine full size test panels. The mid-span deflection was found to be sensitive to the number of nails attaching the panel to the sill plate. For one situation, the deflection was reduced by 13 percent when eight additional nails were added to the connection between the cladding and the sill plate. The amount of restraint was found to be greater for studs with a low modulus of elasticity than for those with higher values. The additional restraint decreased with increasing lateral load because of non-linear behaviour. The effect of axial stud loads upon the connection was not investigated.

The FINWALL program was obtained by BRANZ from Forest Products Lab for the NAFI wall research project (Deam, 1993). Unfortunately it was not able to be used because of inadequate documentation and because Polensek, its developer, had died. Following similar principles, Deam developed a replacement program, LTF-WALL. This was enhanced by including a finite element representation based on Buchanan's (1986) non-linear timber model as the basis of predicting the system strength when the wall was subjected to high axial compression loads. A simpler analytical model was shown to give reasonable accuracy at the moderate levels of axial compression loads anticipated in New Zealand. Axial tension was ignored for the NAFI project because steel 'cyclone tie-rods' were commonly used to resist wind uplift in the high uplift cyclone regions of Australia.

2.2 Analytical Axial and Face Loaded Stud Model

The analytical stud model, which was developed by Deam (1993) to predict the lateral deflection of a composite stud and sheathing element subjected to combined face and axial loading, was extended to account for the end conditions normally found in light timber framed construction. The analytical model gave mid-height deflections for 90 x 35 mm studs which were within 1 mm of deflections predicted using the non-linear LTF-WALL finite element model for compressive axial loads of less than 15 kN (Deam 1993). The stud model developed by Deam assumes that the stud is perfectly elastic and that the stiffness of the composite cladding and stud is uniform over the full height of the stud.

The analytical model for the investigation described herein was developed specifically to predict the response of a single stud, rather than that of a stud within a wall system, because the stiffness is not significantly affected by load sharing between adjacent studs. Strength is more dependent upon adjacent studs because the failure of one stud does not cause the whole system to fail to resist the applied load.

The stud was modelled as a simple beam-column (Figure 1) of height, h, and stiffness, EI, which was symmetric about its mid-height. A lateral line load, ws, was used to represent the uniform face pressure, w, multiplied by the stud spacing, s. An axial load, P, (compressive or tensile) was applied to both ends at a distance, e, from the centre of area of the stud. The neutral axis for the composite stud section was offset by distance ε from the centre of area (ε could also be used to apply additional eccentricity in order to model edge defects such as knots or saw cuts in the stud). In Figure 1(c) the bending moment due to the line load is greater than the bending moment due to the eccentric axial load.

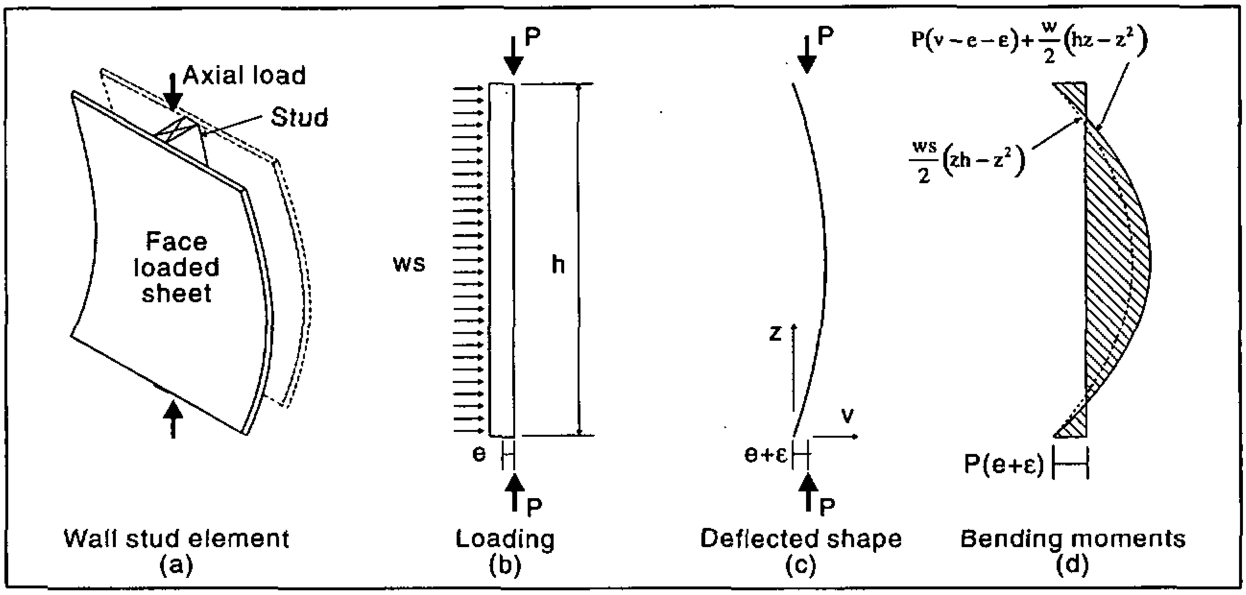

Figure 1. Analytical stud model (Deam 1993).

By equating the Figure 1(d) bending moment to the stud curvature, the lateral deflection, v, is given as (Deam 1993):

$$v = \left(\frac{w}{P\mu^2} - e + \varepsilon\right)\left(\cos\mu z + (\operatorname{cosec}\mu h - \cot\mu h)\sin\mu z - 1\right) + \frac{w}{2P}\left(z^2 - hz\right) \qquad (1)$$

where the multiplier, μ, which makes the length non-dimensional is:

$$\mu = \sqrt{\frac{P}{EI}} \tag{2}$$

The mid-height stud deflection, δ, and stud base rotation, θ, are obtained from Equation 1 as:

$$\delta = \left(\frac{w}{P\mu^2} - e + \varepsilon\right)\left(\frac{1}{\cos 0.5\mu h} - 1\right) - \frac{wh^2}{8P} \tag{3}$$

$$\theta = \left(\frac{w}{P\mu^2} - e + \varepsilon\right)\left(\frac{\mu - \mu\cos\mu h}{\sin\mu h}\right) + \frac{wh}{2P} \tag{4}$$

For tensile axial loads, the eccentricity, e, of the axial load will commonly be half of the stud depth, d, with the axial load being applied through a connector attached to one edge of the stud.

For compressive axial loads, the eccentricity changes as the end of the stud rotates. The stud end remains in full contact with the top (and bottom) plate whenever the stud end rotation is less than a critical angle, θ_{cr}. The contact area reduces (Figure 2(b)) as the rotation increases beyond θ_{cr} and the top plate crushes because it is loaded perpendicular to the grain. (The perpendicular to grain elastic modulus, E_p, for timber is approximately 0.05 to 0.1 times the size of the parallel to grain modulus, E.)

Deam (1993) proposed a simple model for the stud to plate connection (Figure 2) which assumed the stress increased linearly across the contact area (Figure 2(b)). The rotation of the lower surface relative to the upper surface was modelled using the beam equation. The critical angle was defined as that at which the compression stress at one face was zero. The axial load eccentricity, e (Figure 2), was defined in terms of the axial load, P, the stud depth, d, and width, b, and the top plate thickness, t, and modulus of elasticity, E_p.

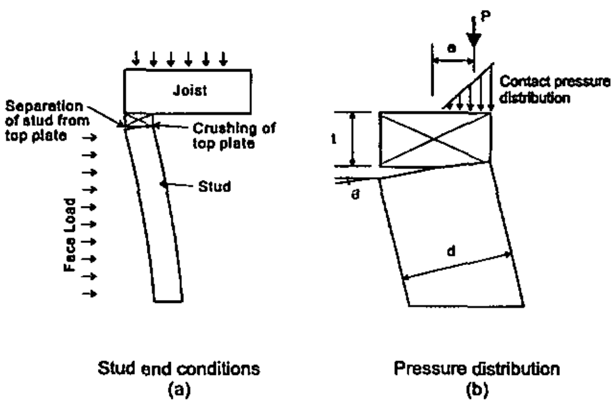

$$e = \frac{cE_p bd^3}{12t}\theta \quad \text{where} \quad c = 1 \qquad \theta \le \theta_c$$

$$c = 0.5(a+1)(1-2a)^2 \qquad \theta > \theta_c$$

$$\text{and} \quad a = 0.5 - \sqrt{\theta_c/\theta} \qquad \theta_c = \frac{2Pt}{E_p bd^2}$$

Figure 2. Stud end model (Deam 1993).

The Figure 2 expressions assume that the axial load is applied/resisted by a rigid component material, beyond the outer face of the plate, at both ends. In practice the load will often be applied to the top of the stud by a timber joist or truss chord which is itself loaded perpendicular to the grain and is located somewhere between two adjacent studs. The additional crushing of the joist and the twisting of the top plate are able to be simulated in the stud model by increasing the top plate thickness or reducing E_p. The nails between the top plate and the stud and between the sheathing and the top plate are ignored because the effect is the same when the top plate rotates relative to the support as it is if it remains stationary and the stud rotates. (The top plate was observed to remain stationary in most of the experimental testing.)

Both parts of the analytical model were programmed into an Excel spreadsheet. An iterative (secant) method was used to find the eccentricity, e, at the stud end for given face and compressive axial loads by minimising the difference between the rotation calculated using Equation 4 and that calculated using the Figure 2 equations.

For a fully composite section the neutral axis offset and the stiffness may be calculated using the traditional transformed area method. These were calculated for a range of sheet widths and sheet elastic modulii and plotted in Figure 3 for a gypsum plasterboard sheet (with an elastic modulus of 1 GPa) attached to the rear face. The neutral axis shifts toward the rear face (Figure 3) when the front sheet is absent (i.e. the elastic modulus or MOE = 0) and towards the front face as the elastic modulus of the front sheet is increased. The maximum elastic modulus of 6 GPa given in Figure 3 is for fibre cement board. The stiffness of the composite system is normalised by dividing it by the stiffness of the stud. Both plots assume that the sheets are rigidly attached to the stud. Often nailslip between the sheet and stud and 'shear lag' effects in the sheet material reduce the amount of composite action. This reduction can be approximated by reducing the sheet width to an 'effective width' for use in the model. The effective width is found by adjusting it until the predicted stiffness matches the measured stiffness for a system.

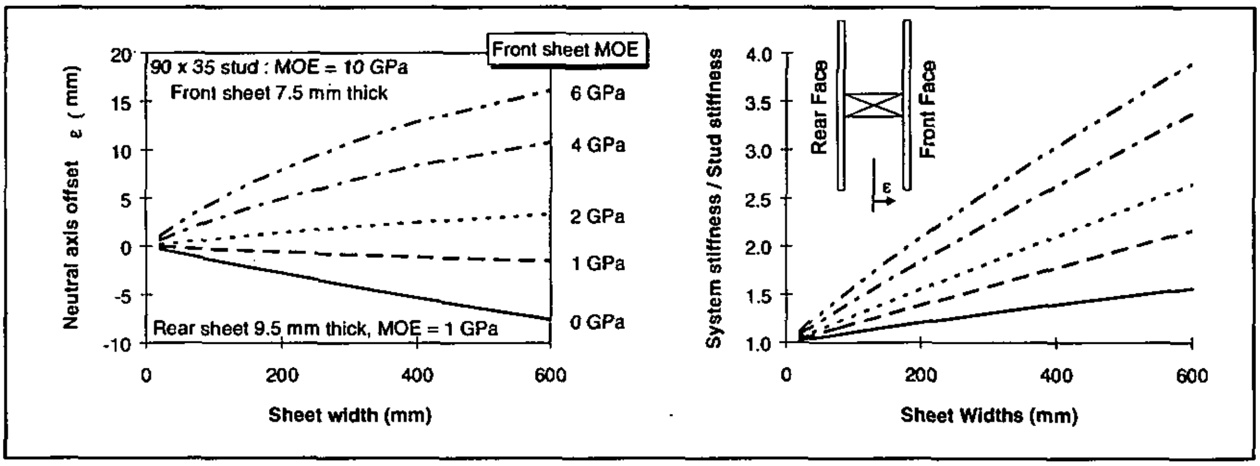

Figure 3. Neutral axis offset and stiffness of composite stud and sheet.

2.3 Experimental Details

This investigation was designed to enable experimental results to be compared with a theoretical model developed in parallel with the experimental work so that the stiffness enhancement of the wall systems due to the presence of sheathings could be analytically determined. Seven combined axial and face load tests were performed on 2.4m high timber studs, lined on one side with 9.5mm gypsum plasterboard. Some specimens were also clad with 7.5 mm fibre-cement sheets as detailed in Table 1. The walls were constructed and tested with the specimen in a horizontal orientation to simplify the vacuum chamber construction. Full construction details are given in Figure 4a. The stud axial load was either applied directly above the stud ("axial") or eccentrically, 150 mm to the side of the stud ("eccentric").

Table 1 Investigation 1 Test Specimen Property Summary

Specimen	Axial Load	Load Type	Fibre-cement Sheet Present?	Notes
S1T1	Tension	Axial	Yes	
S1T2	Tension	Axial	No	
S1T3	Compression	Axial	Yes	
S1T4	Compression	Axial	No	
S1T5				Not tested
S1T6	Compression	Axial	No	
S1T7	Compression	Eccentric	No	
S1T8	Compression	Eccentric	No	

2.3.1 Construction Details

The 2.42 m long specimens had 600 mm wide top and bottom plates gun-nailed to a single stud using two 90 x 3.33 mm coated gun nails at each end.

All timber was kiln dried 90 x 35 mm No 1 framing grade radiata pine which had been stored in the laboratory for three months before testing. Details of the nailing of the gypsum plasterboard and fibre-cement board sheets to the timber frame are given in Figure 4a. There was a 10 mm gap between the ends of the sheets and the bottom of the bottom plate. The same gap existed at the top of the wall specimens.

Axial load was applied to the test specimens through a 150 x 50 mm (nominal) timber stub, as shown in Figure 4a. This was intended to simulate truss loading as indicated in Figure 13. For tension tests the stub was strapped to the sheathing face of the test specimens using short lengths of blocking, as shown in Figure 4a. For tension tests only, a similar detail was used at the other end of the test walls, as shown in Figure 4b. A strong connection was used for the specimens to prevent tension failure at the end connections. However, Figure 13 shows that a strong tension connection is not used in practice. This was investigated further in this work and is reported in Section 3.

2.3.2 Loading

The specimens were mounted above a vacuum chamber (Figure 4c). Polythene was used to seal the vacuum chamber to the specimen without restraining specimen movement. Sealing details of the ends of the specimens are shown in Figure 4b. During testing, air was evacuated from the vacuum chamber using a centrifugal air pump. The reaction force created by the vacuum was restrained by props placed beneath the ends of the top and bottom plates (Figure 4a and Figure 4d). For test walls without external sheathings, the vacuum was applied to the internal lining. This represents the situation where the external sheathing is permeable (eg rain-screen type) and adds no structural strength to the system.

The vacuum was only applied to a 352 mm wide strip of the 600 mm wide sheet so that the sheathing was not subjected to more stress than it would be if it was part of a multi-stud wall. Vacuums quoted in the remainder of this report (i.e. in Figures 7 to 12) are the equivalent multi-stud wall vacuum obtained by multiplying the measured test pressure by 352/600.

The seals were held to the gypsum plasterboard or fibre-cement board with short lengths of battens (Figure 4c). Where both fibre-cement board and gypsum plasterboard were used, bolts connecting the two at 600 mm centres ensured that both sheets deflected the same amount.

Axial load was applied to the specimens using an actuator as shown in Figure 4b. The 150 x 50 loading beam was forced to remain near vertical by the wall tie back system. The purpose of this was to simulate trusses remaining horizontal in practice. A rigidly restrained steel beam beneath the bottom plate simulated the foundation condition (Figure 4a and Figure 4d).

Two tests were performed with the applied axial load eccentric to the stud (Figure 4e). An additional stud was used and the axial load in this additional stud measured. The axial load in the test stud was calculated by subtracting the load in the additional stud from the total applied load.

Buildings designed to NZS 3604 (SNZ 1990) in very high wind regions could expect to be exposed to wind pressures of up to 1.5 kPa. Extraordinary circumstances (such as funneling effects caused by the local topography) may mean that the pressures are greater than 1.5 kPa. The maximim gravity loads expected on studs spaced at 600mm centres in buildings designed to NZS 3604 are approximately 4.75 kN per stud from dead weight and up to 2.6 kN per stud from live loading, a total of 7.35 kN. To cover these expected load levels in the field, the test specimens were loaded up to 10 kN axially in compression and 6 kPa in bending. Uplift forces on studs under wind loading could be expected to be up to 7 kN per stud in very high wind exposure areas. In the tests the specimens were loaded in tension up to 10 kN.

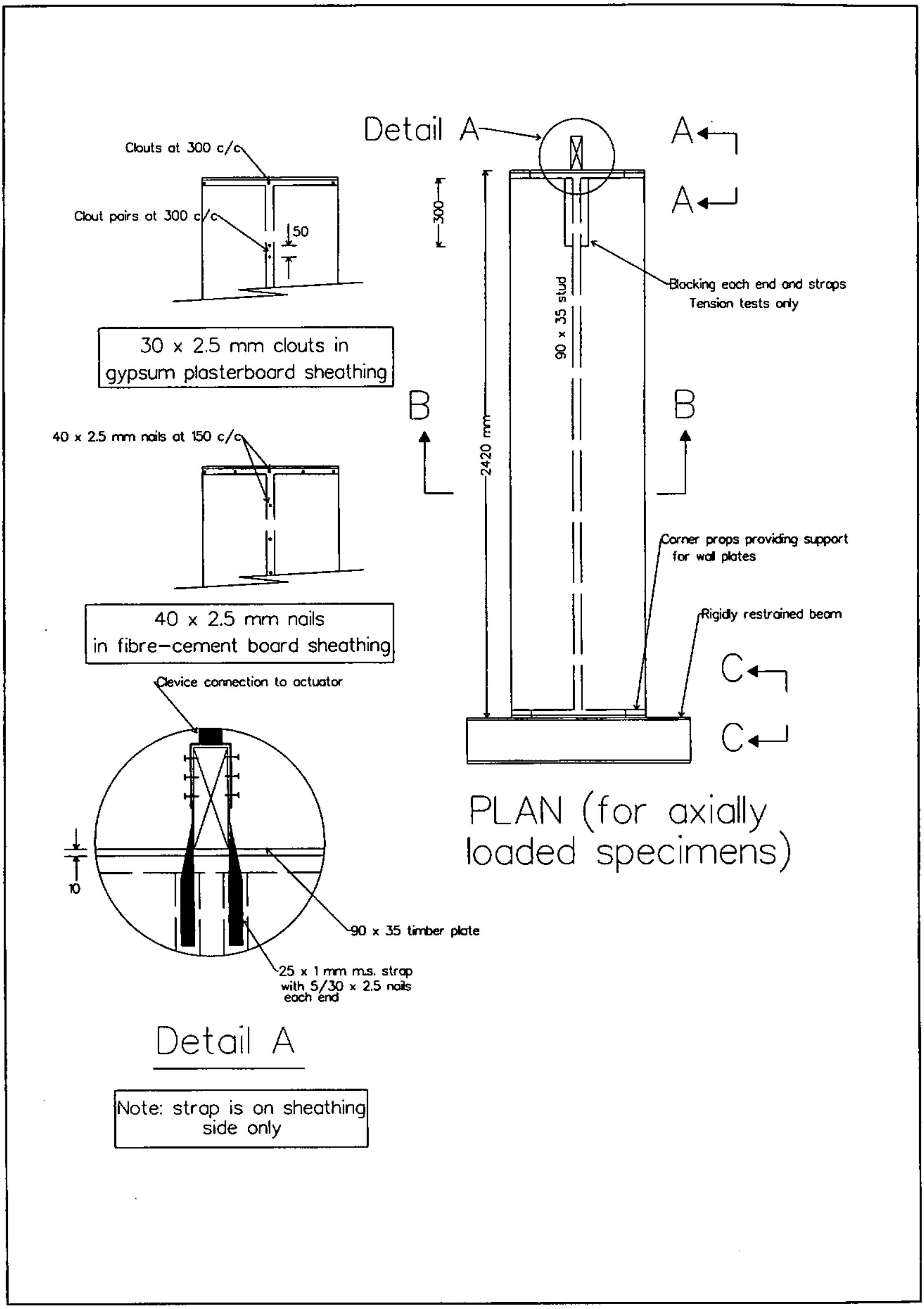

Figure 4a. Investigation 1 test setup.

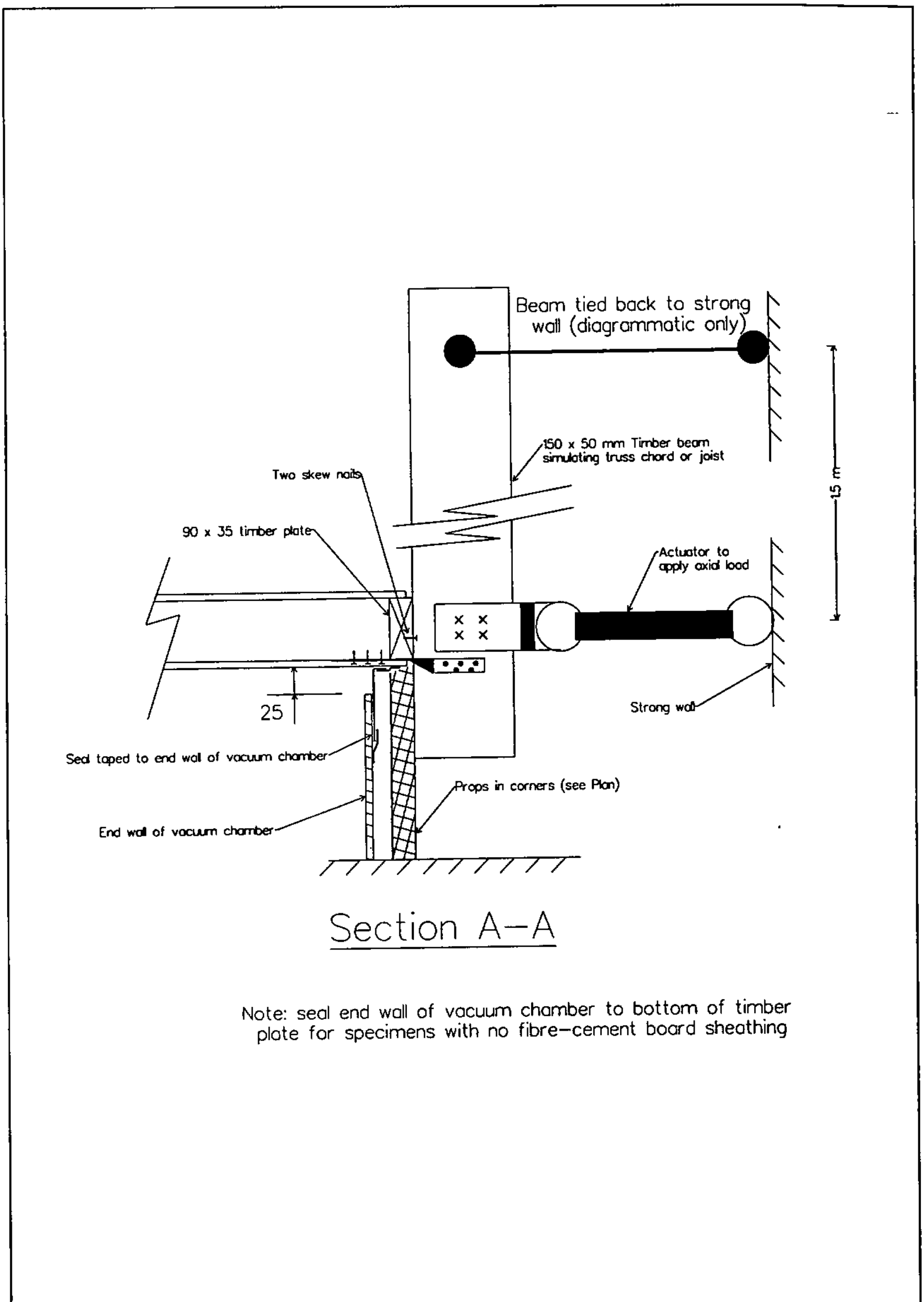

Figure 4b. Investigation 1 test setup (contd).

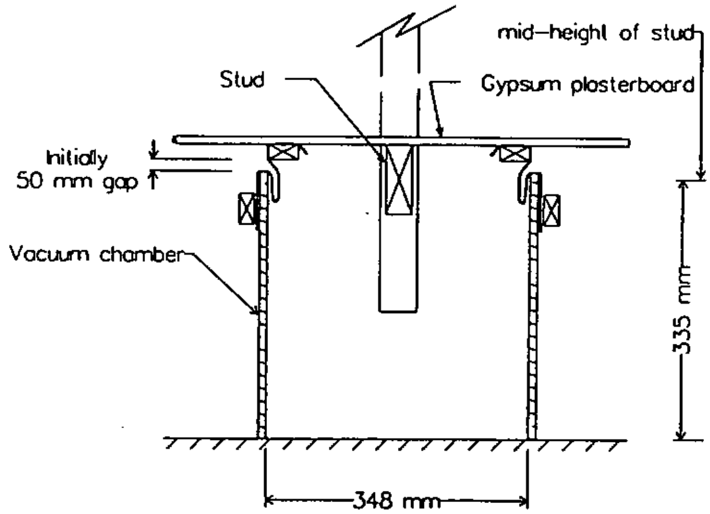

Section B–B for axially loaded specimens
(specimens with no fibre–cement board sheathing)

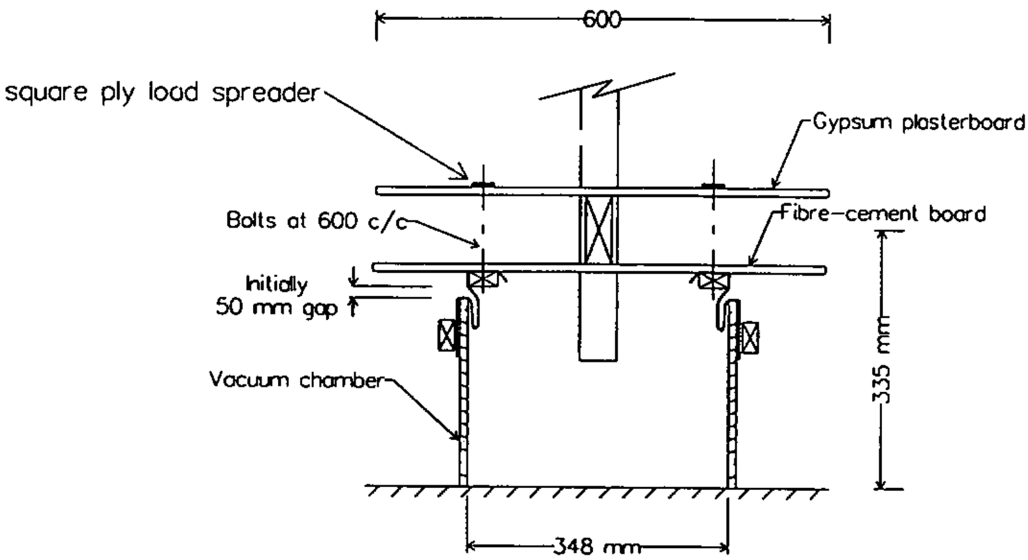

Section B–B for axially loaded specimens
(specimens with fibre–cement board sheathing)

Figure 4c. Investigation 1 test setup (contd).

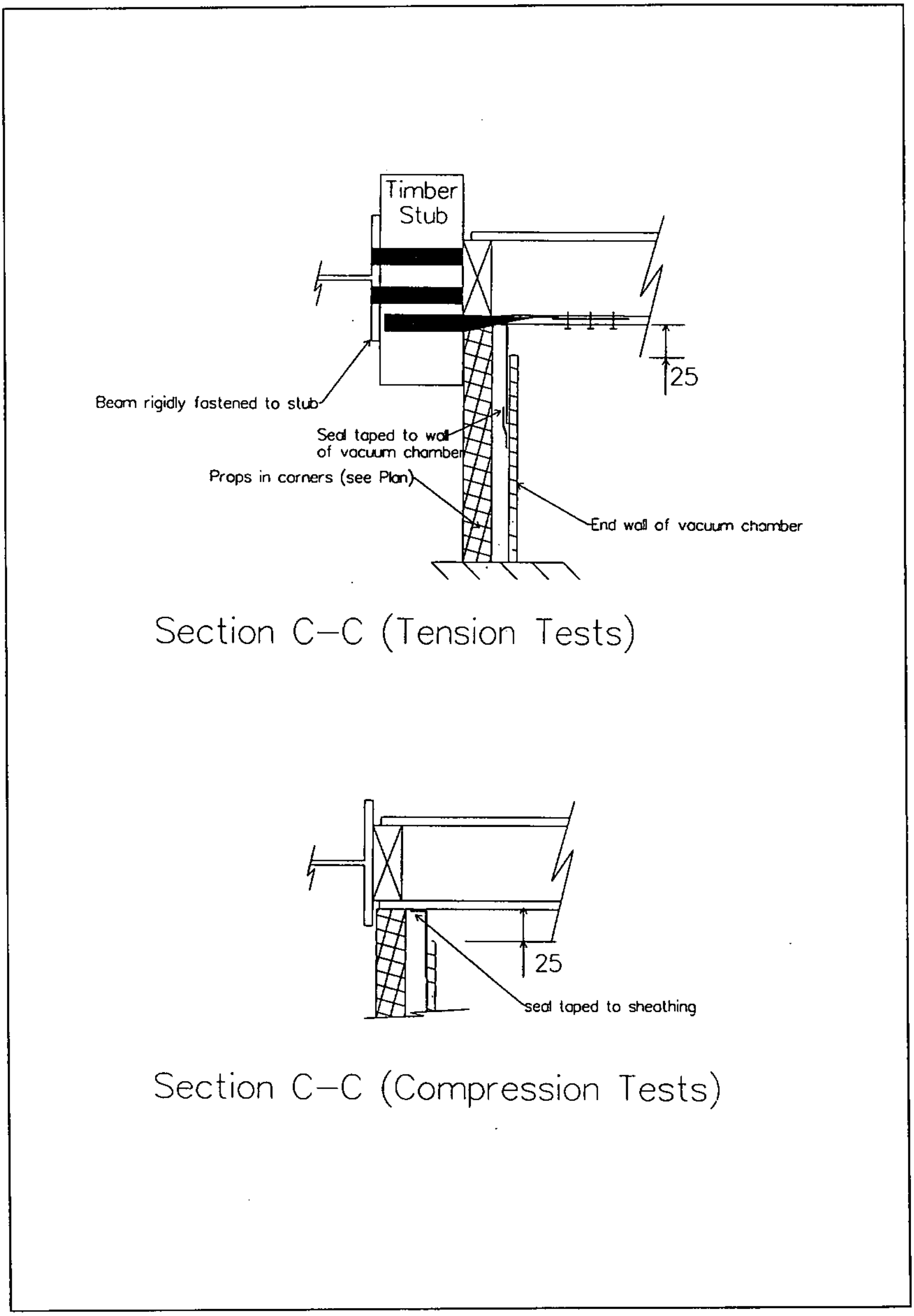

Figure 4d. Investigation 1 test setup (contd).

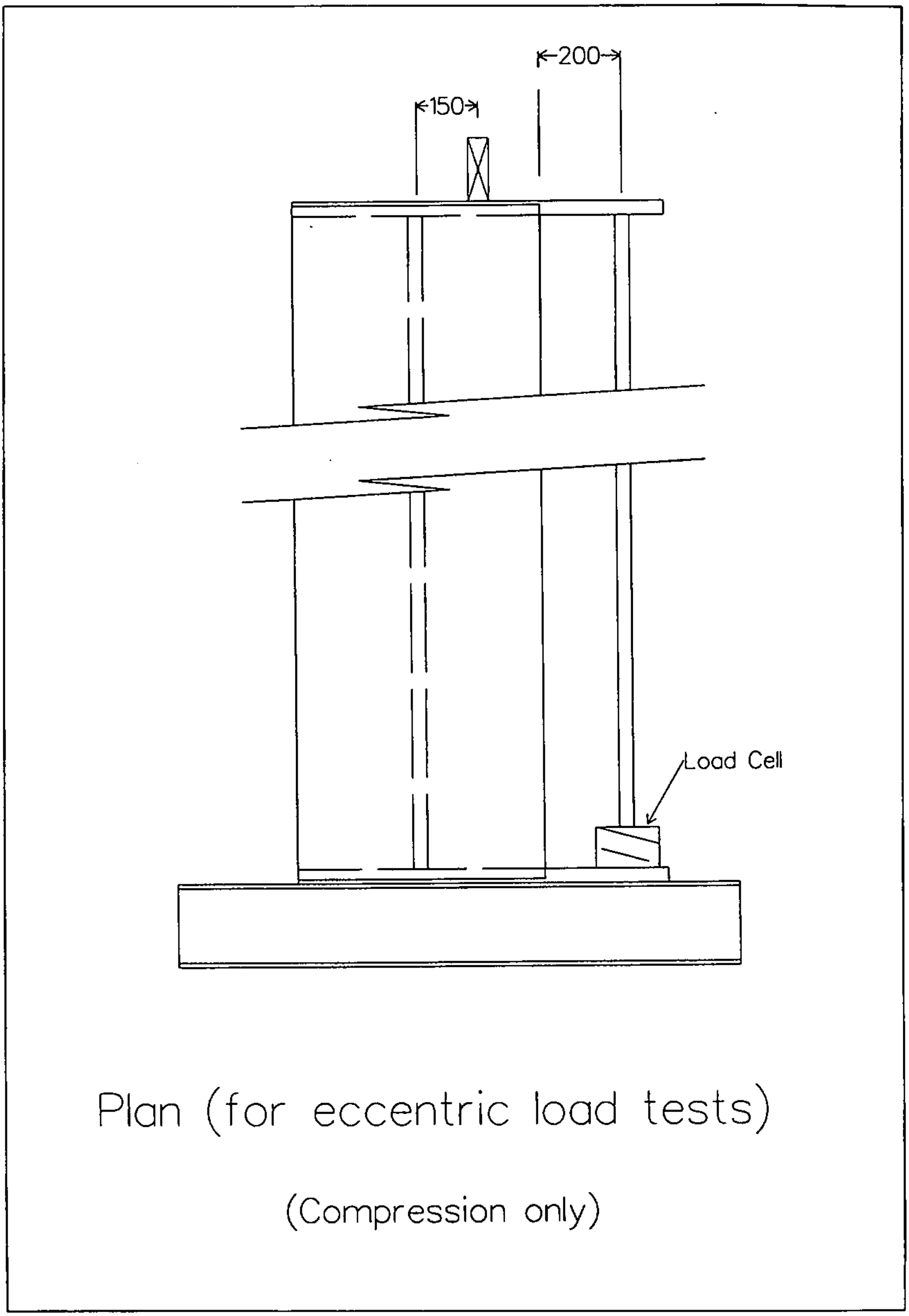

Figure 4e. Investigation 1 test setup (contd).

2.3.3 Load Regime

As the wall specimens were tested in a horizontal orientation, they were weighed before testing commenced. The vacuum load applied was in the same direction, and thus additional to the self weight loading.

The general load regime used on the test specimens is given below. A different load regime was used for Specimen 4, which is separately described. Vacuum was applied at the rate of approximately 2 kPa per minute and axial load at 5 kN per minute.

(a) <u>Compression Tests</u>

<u>Step 1</u>
With zero axial load, a 1.5 kPa vacuum was applied to enable the initial system stiffness to be compared with the single stud stiffness (Table 2).

<u>Step 2</u>
A 10 kN compressive axial load was applied and then a vacuum to 2.5 kPa while the axial load was maintained.

<u>Step 3</u>
Step 2 was repeated for axial loads of 7 kN, 4 kN, 2 kN and 0 kN.

<u>Step 4</u>
A selected axial load was applied and then a vacuum was applied to failure or 6 kPa, whichever happened first.

(b) <u>Tension Tests</u>
The procedure was the same as for the compression tests but the axial loads were tension loads and the order of loading for Steps 2 and 3 was from low to high (i.e., 0, 2, 4, then 10 kN tensile).

(c) <u>Specimen 4</u>
Only Step 4 was followed.

2.3.4 Instrumentation

The applied load was monitored by a 20 kN load cell calibrated within BS 1610 (BSI, 1985) Grade 1 accuracy. For tests 7 and 8 the load in the additional stud was monitored by a 10 kN load cell also calibrated within BS 1610 Grade 1. Air was evacuated from the vacuum box with a centrifugal fan, and the vacuum was monitored with both 5kPa and 25 kPa Schaevitz electric vacuum gauges. These gauges were calibrated within 0.05 kPa accuracy.

Deflections were measured with linear potentiometers at the locations shown in Figure 5. Gauges 1 and 2 measured the movement of the top plate relative to the stud to ascertain the degree of top plate rotation and stud crushing. Slips of the sheets relative to the studs were measured with Gauges 3 and 4. Gauges 5 to 8 were provided for the same purpose as gauges 1 to 4 except they were located near the bottom plate. Gauges 9 to 13 measured vertical movement at locations shown in Figure 5. Gauges

1 to 8 were either 20 or 50 mm potentiometers, (accuracy ± 0.3 mm) while Gauges 9 to 12 were 100 mm potentiometers (accuracy ± 0.4 mm).

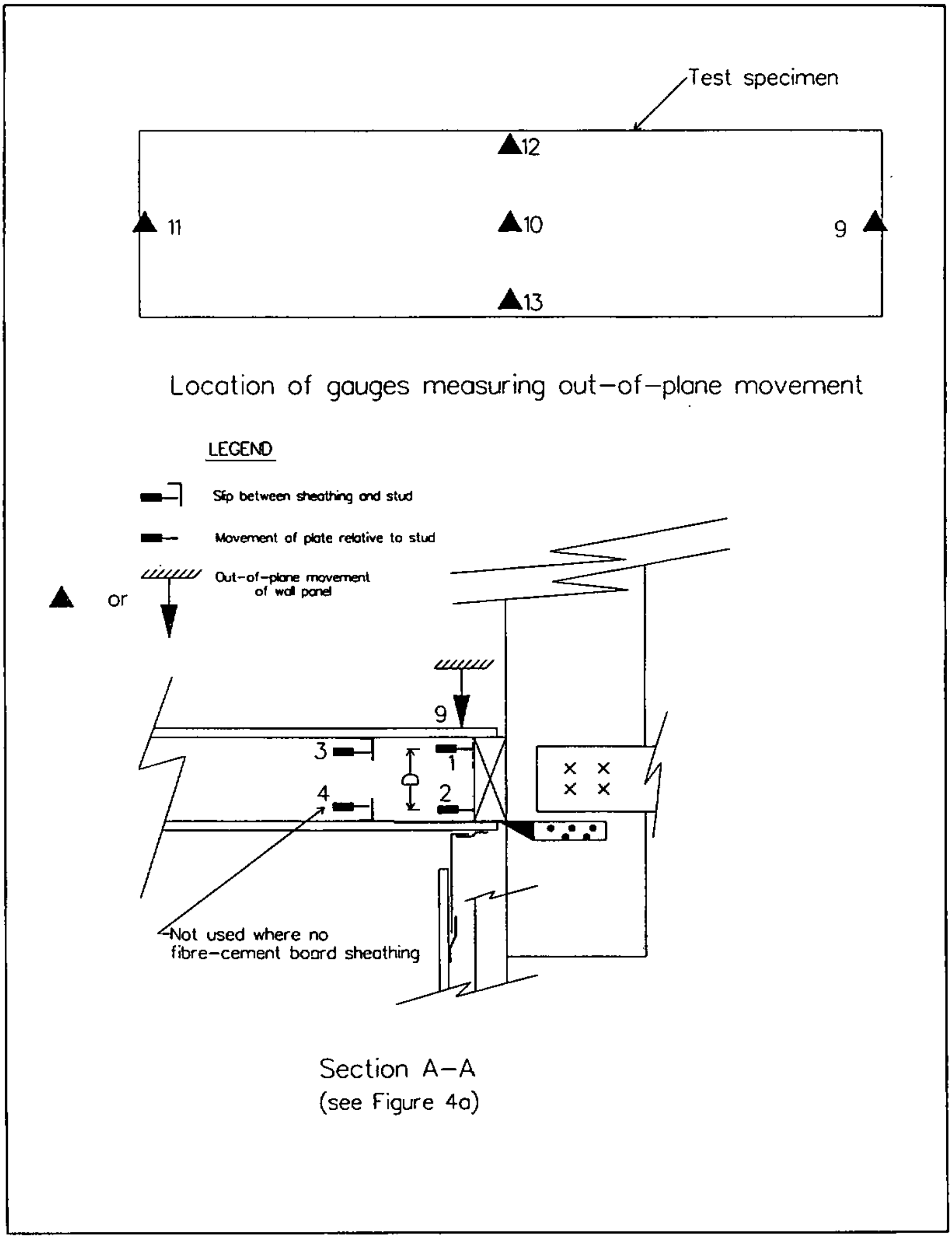

Figure 5. Instrumentation for the Investigation 1 tests.

2.3.5 Measurement of Stud Elastic Modulus

The elastic moduli of the timber studs used for investigation 1 were measured by applying 2-point loading up to 1.5 kN force using the BRANZ standard test ST18 (which is a variation of AS/NZS 4063 [SNZ, 1992b]). Results are the same as would be produced by AS/NZS 4063. Test setup details are shown in Figure 6 and results are presented in Table 2. The studs were tested in the same direction as the vacuum imposed loadings in Table 1.

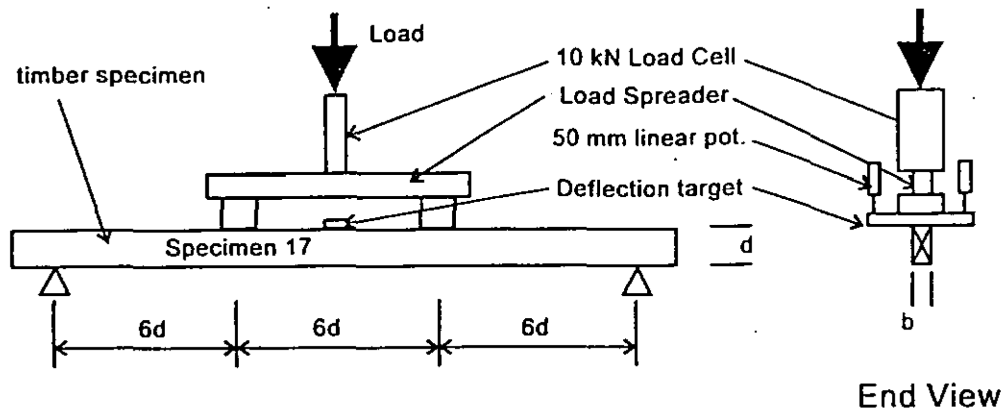

Figure 6. Test setup for 2-point bending test.

2.4 Results

2.4.1 Individual Stud Elastic Moduli

Results of the 2-point bend tests to determine the elastic moduli of the timber studs before installation in the vacuum chamber are presented in Table 2.

Table 2 Stiffness and Modulus of Elasticity of the Individual Studs

Specimen Number	Bending Stiffness (kN/mm)	Elastic Modulus (GPa)
S1T1	0.384	11.86
S1T2	0.344	10.63
S1T3	0.390	12.03
S1T4	0.331	10.21
S1T5	0.318	9.80
S1T6	0.392	12.09
S1T7	0.343	10.59
S1T8	0.325	10.01

2.4.2 Pressure Test Results and Comparison with Analytical Model

Little damage was observed in the specimens during testing. Specimens S1T1, S1T2 and S1T3 showed no failure or distress even at the maximum vacuum of 6 kPa that the equipment was able to impose. The remaining specimens developed a crack in the gypsum plasterboard, parallel to and near the stud, at vacuums between 5.6 and 6.0 kPa.

An example match between the analytical stud model and the experimental results is plotted in Figure 7. The predicted responses are plotted with lines and the experimentally measured responses are plotted as individual '+' points. For clarity, the responses for different axial loads are translated horizontally. The origin for each axial load is indicated on the plot by a vertical line extending between 0 and 0.5 kPa vacuum. The composite stud stiffness, eccentricity and top plate elastic modulus were all adjusted to obtain the best match between the model and the experimental response.

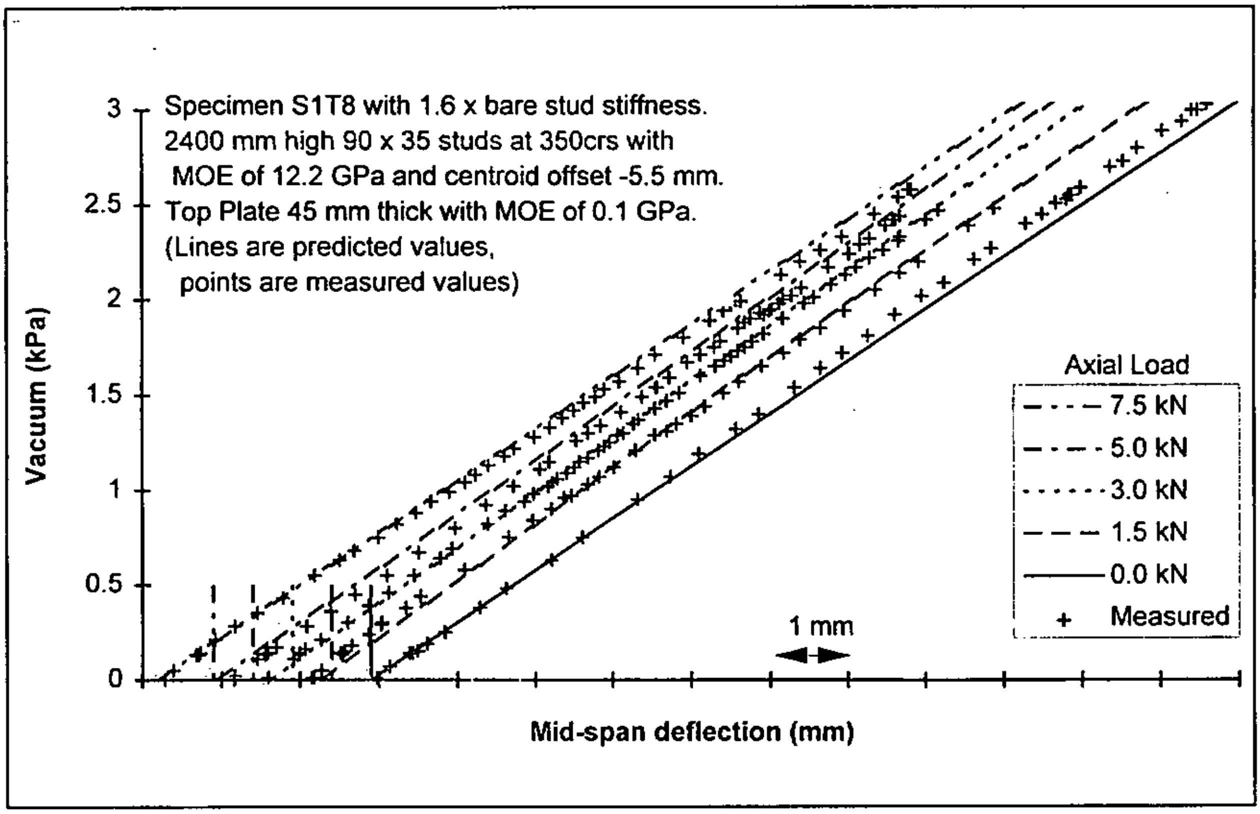

Figure 7. Predicted and experimental results for Specimen S1T8.

The vacuum is plotted against the mid-span deflection for the other specimens in Figures 8 to 12 along with the Section 2.2 stud model predictions. The experimentally measured responses are given as individual '+' points and the predicted responses are given as continuous or broken lines. The responses for different axial loads are separated on the plot for clarity as described for specimen S1T8. Positive axial loads are compressive and negative axial loads are tensile. The composite stud stiffness, eccentricity and top plate elastic modulus were all adjusted to obtain the best match between the model and the experimental response. The measured elastic modulus of the bare stud was used in the model.

The response of Specimen S1T1, with fibre-cement board on one face and gypsum plasterboard on the other face, is given in Figure 8. The specimen was subjected to five constant axial tension loads with the force applied at an eccentricity of +45 mm from the stud centroid (see Figure 4b for position of loading strap). The upper plot shows that the stiffness of the specimen was initially about four times the bare stud stiffness. The stiffness decreased as the vacuum increased but there was a good match in the initial deformation and stiffness up to about -7 kN (tension). The lower plot also shows that an initial stiffness of 3.5 times was a better match for the response at -10 kN. Also note that because the combined eccentricity is positive, the stud deflects further as the axial load increases when there is no vacuum applied.

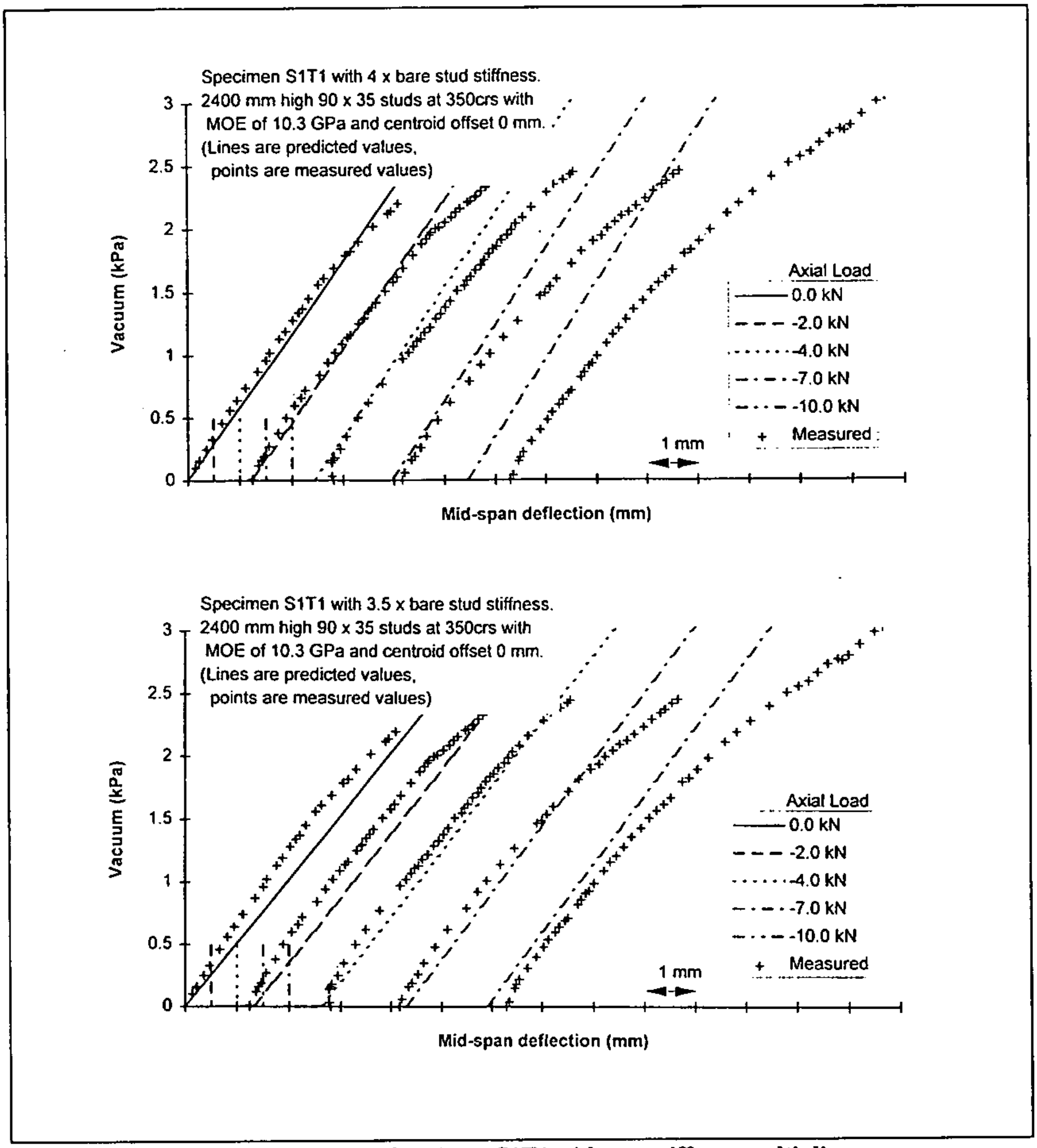

Figure 8. Mid-span responses of Specimen S1T1 with two stiffness multipliers.

Specimen S1T3 was identically constructed to Specimen S1T1 but subjected to compressive axial loading. The response of Specimen S1T3 given in Figure 9 was well predicted for compressive loads of 0 to 7 kN but the stiffness decreased by 13 % at 10 kN. The stiffness decrease was accompanied by 14 mm movement of the neutral axis position.

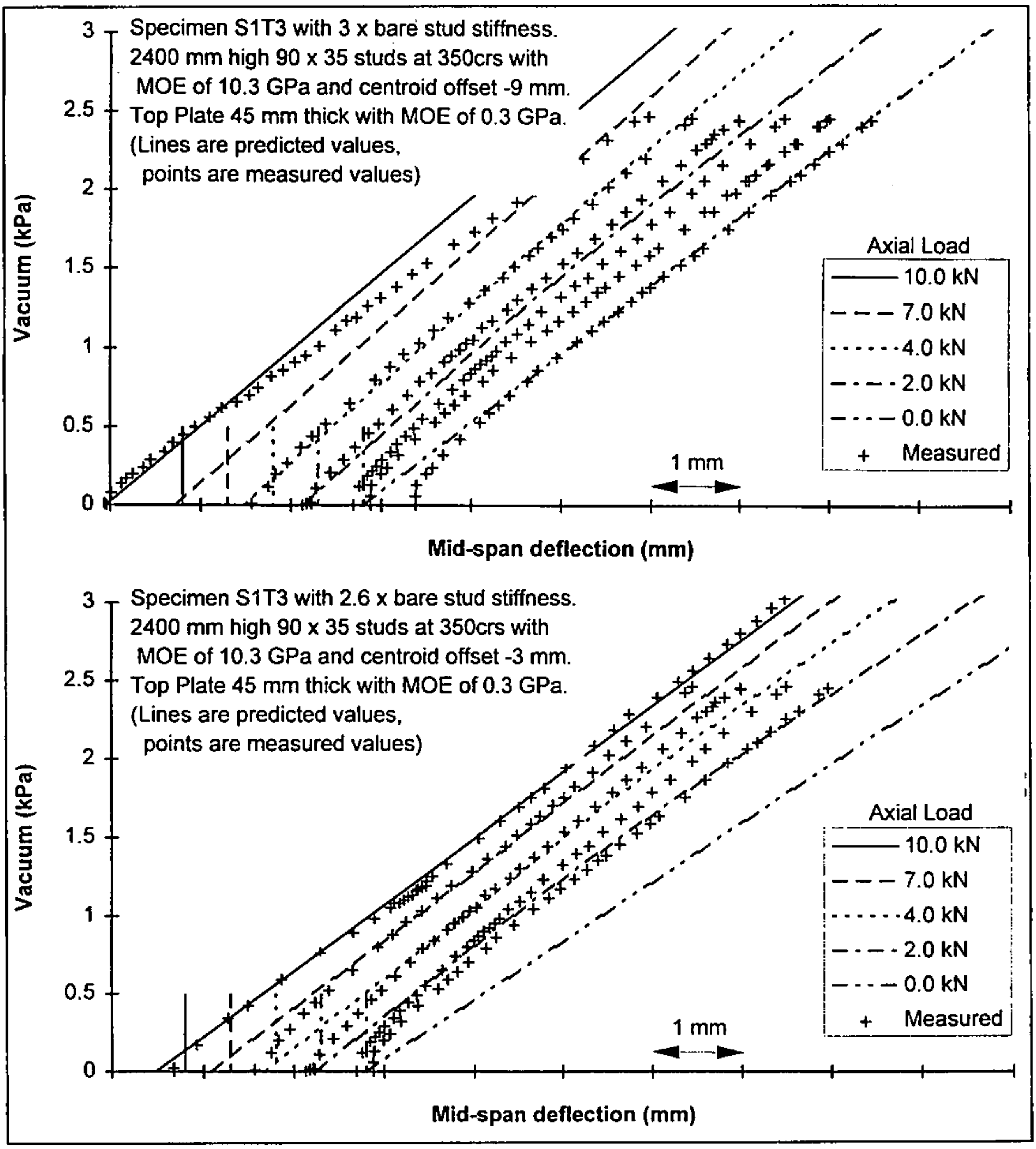

Figure 9. Mid-span responses for Specimen S1T3.

It is of note that the responses were more linear for compressive axial loads than for tensile axial loads. This occurs because, for compressive loads, the axial compression strain opposes the tensile bending strain on the lower face of the stud. This reduces the effectiveness of the sheet material for the compressive load, producing a lower stiffness than with the tensile load.

Specimen S1T2 had gypsum plasterboard on the upper (compression) face and was loaded with a tensile axial load. The response (Figure 10) was more linear than that of Specimen S1T1 with fibre-cement board on the lower (tension) face. This was primarily because the elastic modulus of the gypsum plasterboard was only one sixth that of the fibre-cement board on Specimen S1T1.

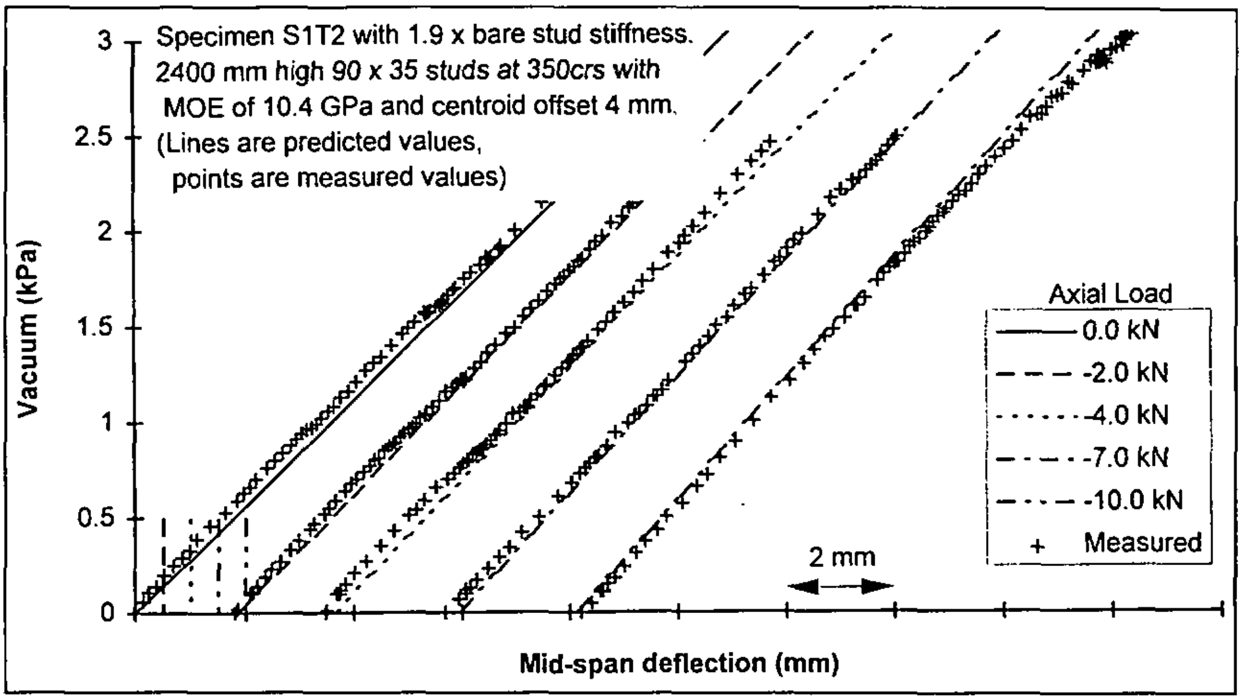

Figure 10. Mid-span responses for Specimen S1T2.

The responses of Specimens S1T4 and S1T6 are given in Figure 11. These specimens had gypsum plasterboard on the upper face and were loaded with a compressive axial load. The Section 2.2 model matched these specimens very well.

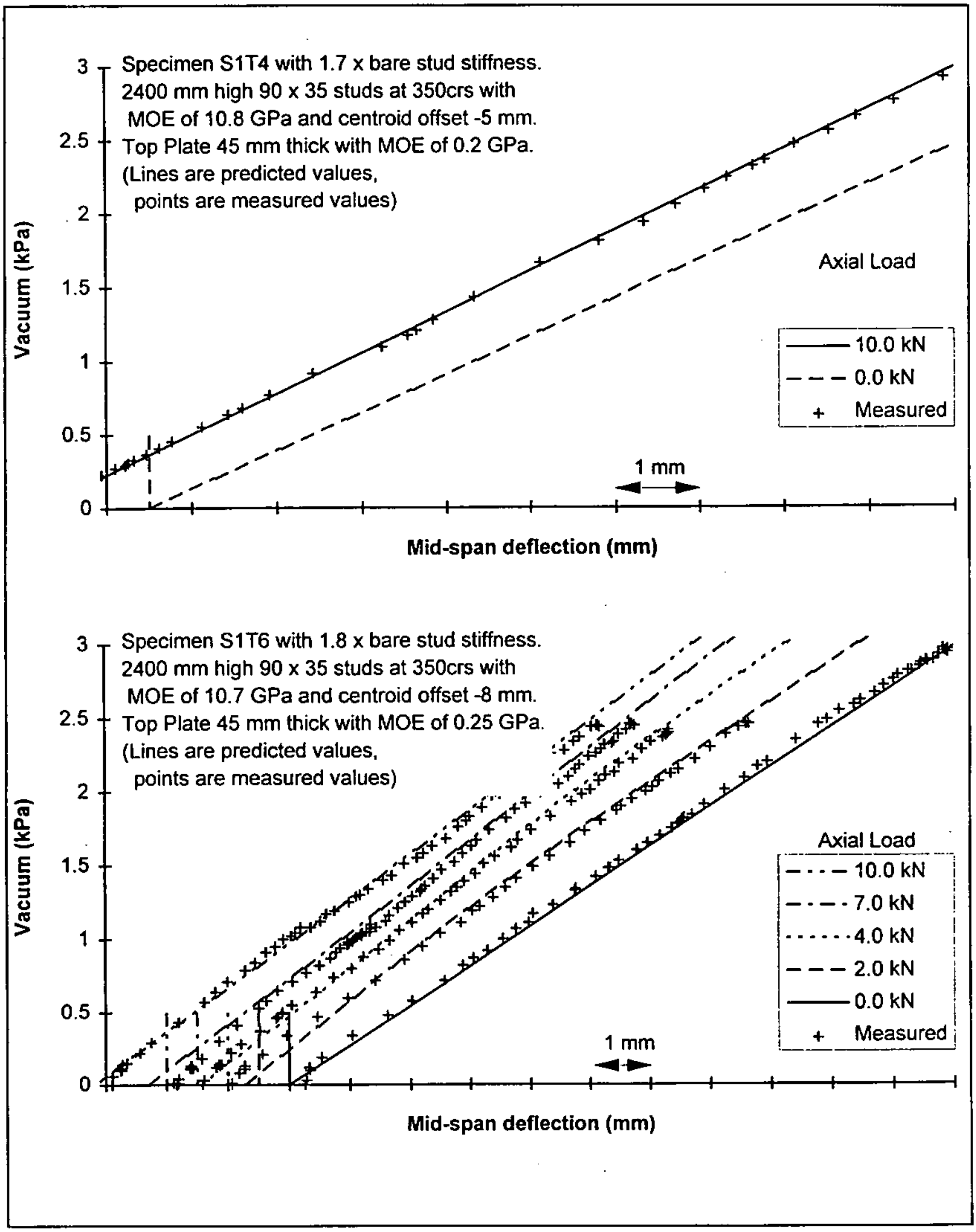

Figure 11. Mid-span responses for Specimens S1T4 and S1T6.

The responses of Specimens S1T7 and S1T8 are given in Figure 12. These specimens had gypsum plasterboard on the upper (compression) face and were loaded with a compressive axial load which was applied to the top plate a quarter of the way between the test stud and an adjacent stud. The model also matched these specimens very well once the top plate elastic modulus was halved to 0.1 GPa (from the 0.2 - 0.3 GPa used for the other specimens).

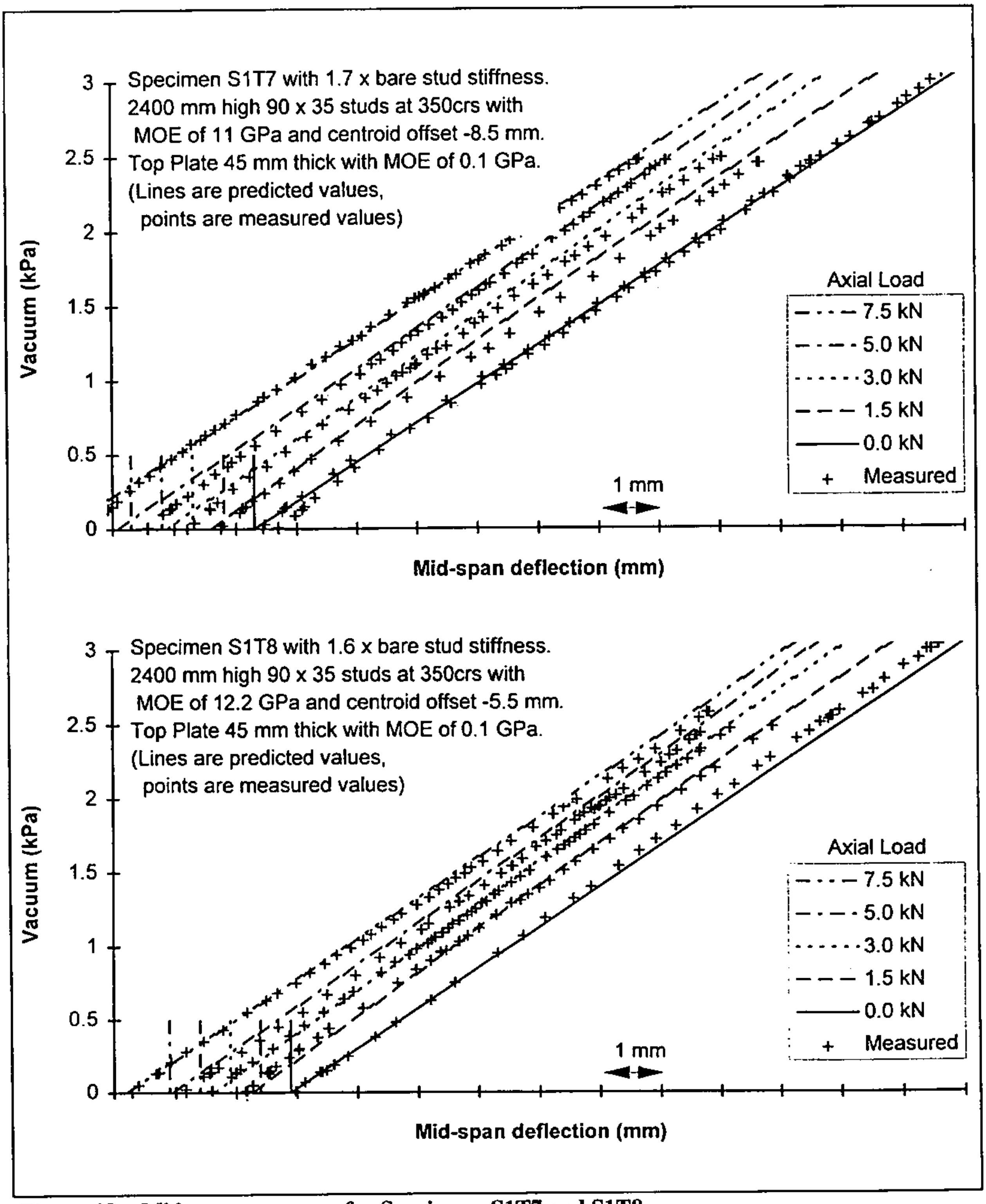

Figure 12. Mid-span responses for Specimens S1T7 and S1T8.

3. Rafter/Top Plate/Stud Connections

3.1 Literature Review

Adequate strength of the connections between rafters and the top framing plate is required to ensure that a load transfer path is available to carry axial tensile loads to wall studs. Surveys of houses constructed according to the New Zealand Code of Practice for Light Timber Framed Buildings not requiring specific design, NZS 3604 (SNZ,1990) and to earlier codes of practice, have shown that the roofs sometimes separate from the walls in extreme winds (Cooney [1980] and Lim [1990]), indicating that the installed skew nail connection between rafter and top plate may not always be adequate. Apart from the addition of the very high wind zone case to NZS 3604 in the 1990 version, the connection requirements were unchanged from the 1984 version.

According to NZS 3604, the connection between rafter and top plate need only be two skewed 100 x 3.75 mm nails for most houses in low and medium wind exposure zones. Additional "Z" shaped wire dogs are required in certain cases in the high wind zone and for houses with large rafter spans or spacings in the lighter wind zones (see Appendix A). The stud to top plate connection need only be two 100 x 3.75 mm nails (end nailed) except that, in high wind exposure light roofs where the span exceeds 7.2m, "U" shaped wire dogs or strap connections are additionally required at not more than 900 mm centres. Examples of those connections are shown in Figure 13.

The strength of the connections is not readily available from literature. The contributing area upper limits for such connections were calculated (see Appendix A) and multiplied by the design wind pressures for the four wind exposure conditions of NZS 3604 (SNZ,1990) to determine the design loads.

To investigate whether a problem of inadequate connector strengths existed, tests were performed as outlined in Table 3. Simulations of the joints were constructed and tested as shown in Figure 14.

3.2 Experimental Details

3.2.1 Construction Details

The specimens were constructed to represent the situation of roofs of structures with exterior brick veneers. This is a 'worst case scenario', as in this case there was no exterior sheet lining providing assistance to the nailed connection between the top plate and the studs.

All timber members (ie rafter, top plate and stud members) in this test series were nominal 100 x 50 No. 1 framing at a moisture content of approximately 15%.

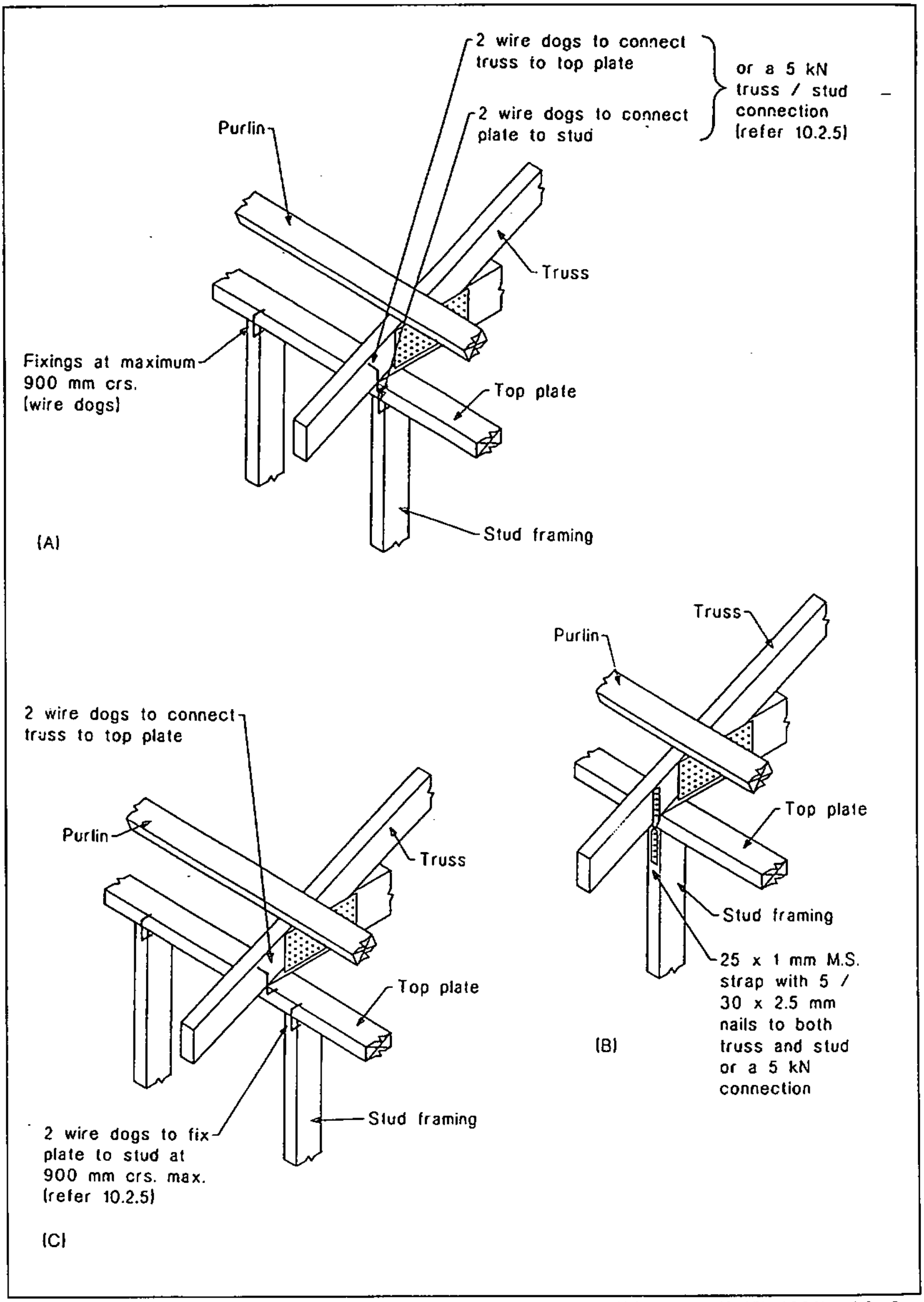

Figure 13. Truss/top plate connections (reproduced from MP3600:Part 1 (SNZ, 1992) with the permission of Standards New Zealand).

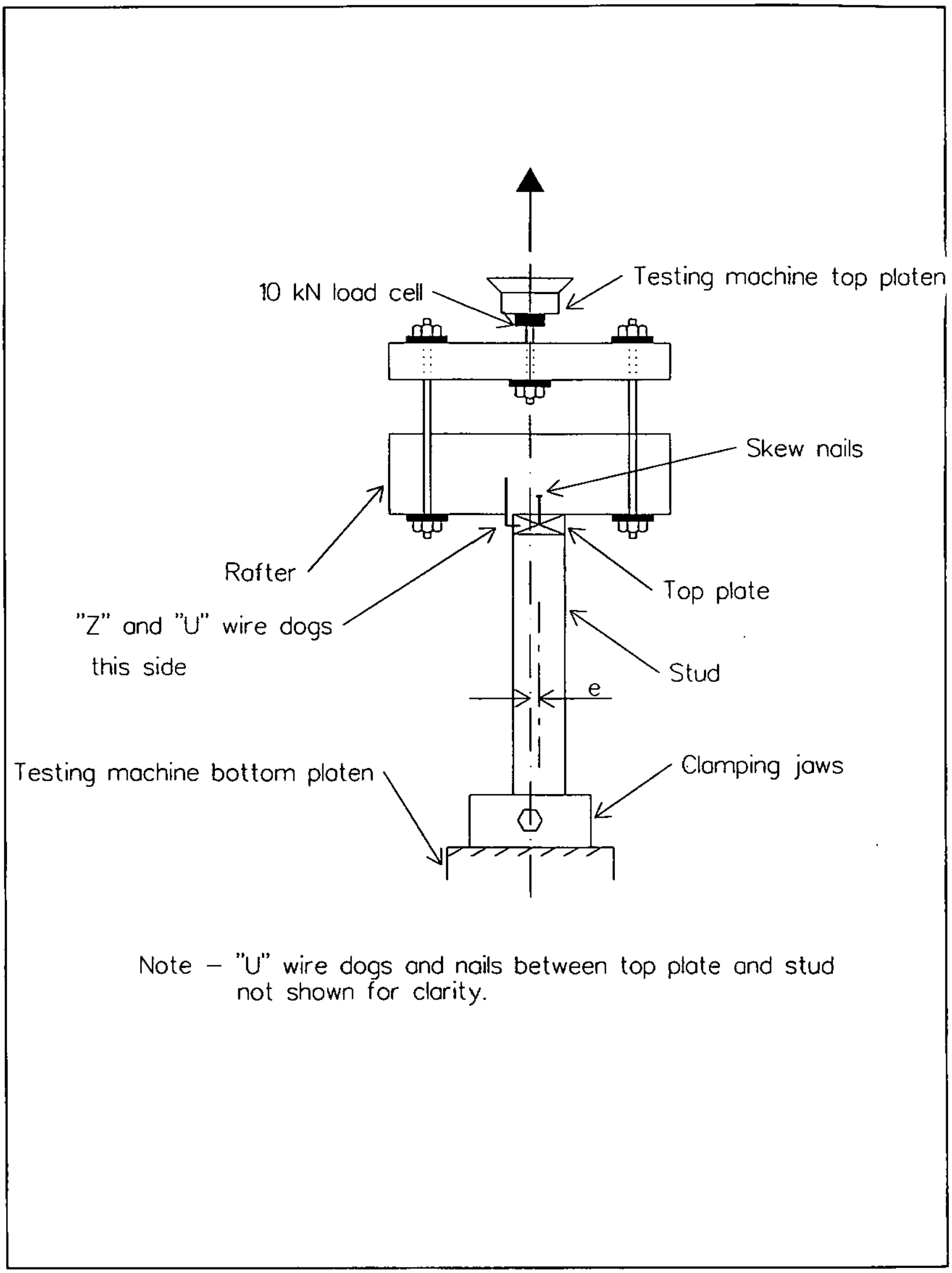

Figure 14. Investigation 2 test setup.

Table 3 Tension Separation Tests on Rafter/Top plate/Stud Connection Specimens

Test Type	Rafter to top plate connection	Top plate to stud connection
A	Two skewed 100 x 3.75 mm nails.	Two 100 x 3.75 end nails.
B	As per Test A plus: two "Z" shaped nails (wire dogs), one left handed and one right handed.	As per Test A
C	As per Test B.	As per Test A, plus two "U" shaped nails (wire dogs), (i.e., one either side of the plate).

3.2.2 Loading

The tests were performed in the BRANZ Universal Testing Machine using a loading rate of 1 kN per minute. The eccentricity, e, (shown in Figure 14) was varied so that the simulated rafter lifted vertically from the top plate during testing, and did not rotate. This was generally accomplished with reasonable success, except for specimens Bl and B2 which rotated significantly, (the vertical movement at the right hand side of the top plate being twice that at the left hand side). The measured strengths were compared with the predicted demands for various roof types and exposures calculated in Appendix A.

3.2.3 Instrumentation

The applied load was monitored directly from the output of the Universal Testing Machine. While deflection was not considered an important test parameter, the opening of the joints was measured using the displacement output from the test machine.

3.3 Results

Results are given in Table 4.

By comparison of Tests A and B it can be seen that the addition of the "Z" shaped wire dogs added little to the stiffness and strength of the system. However the addition of "U" shaped wire dogs significantly strengthened and stiffened the joint. It would appear that the skew nail connection between the rafter and top plate is about equal in strength to the end nailing of the top plate to the stud (the latter joint may be strengthened by the presence of wall sheathing.) Thus, both the rafter to top plate and top plate to stud connection need to be strengthened to increase the strength of the total system, as was done in the Type C tests.

A comparison of the predicted design loads from Appendix A with the measured strengths in Table 4 shows that:

1. Light framed roof rafters fixed to the top plate with 2 skew nails in low and medium wind exposures and within the span and spacing limits of NZS 3604 (SNZ, 1990) are satisfactory.
2. Light framed roof rafters fixed to the top plate with 2 skew nails plus 2 wire dogs in a low wind exposure and within the span and spacing limitations of NZS 3604 (SNZ, 1990) are satisfactory.
3. Other combinations of NZS 3604 allowable rafter spans and spacings and wind exposures for light roofs are predicted to fail in the ultimate design wind event.

Table 4 Rafter/Top plate/Stud Tension Results

Test Type	Load (kN) at Deflection (mm)				Max. Load (kN) @ Deflection (mm)	Failure Mechanism
	5mm	10mm	15mm	20mm		
A1	2.40	2.39	2.41	-	2.45	Skew nails partially pulled out of plate
					2.5 - 13mm	
A2	2.19	1.77	1.42	-	2.51 @ 2.5mm	
A3	2.59	2.37	2.32	2.06	2.74 @ 6.5mm	End nails pulled through top plate
B1	-	-	-	-	2.39	End nails pulled through top plate
B2	-	-	-	-	2.78	
B3	2.03	2.05	2.24	1.22	2.24 @15mm	As B1 but skew nails also partially pulled out of stud
B4	1.96	2.01	2.04	1.75	2.09 @ 8.5mm	
C1	3.38	4.32	3.33	2.66	4.48 @ 11mm	"U" nails split stud on assembly and pulled out to one side. End nails and skew nails pulled out.
C2	2.57	2.56	2.50	2.18	2.73 @ 6mm	
C3	4.67	5.43	5.46	3.25	5.90 @ 12mm	No splitting on specimen assembly. Top plate split and "Z" nails partially pulled out during test. End nails and skew nails pulled out.

4. Composite Action of Top Plates and Wall Sheathings

4.1 Literature Review

The vertical corner seam joints between the internal and external wall linings were shown to increase the stiffness and strength of the top plate in a NAFI research project conducted by Reardon and Xu (1993). They also investigated the influence of longitudinal contact friction between the two plate components when they were being used in pairs. A good match was obtained between a finite element model and experimental tests of multiple member (composite) top plates simply supported on studs. These composite plates were composed of equal sized members. They were found to have between 2 and 22 percent greater stiffness than the sum of the stiffnesses of the individual components because of the composite action. The effect of the nails used to attach the sheet material to the top plate was not modelled but the experimental results indicated that the nails had a greater effect on the stiffness than the composite action.

Collins (1980) outlined the engineering bases for the plate tables in NZS 3604:1978 (SANZ, 1978). In his investigation, Collins took account of the performance of members used in the practice of the day. He determined that for plates, bending strength was not critical because they were seen to be performing satisfactorily at stresses in excess of what was normally considered acceptable. Also, the load sharing ability of trusses and rafters due to cross-linking of purlins and ceiling framing meant that any excessive deflection of a single truss or rafter was readily redistributed to adjacent members. No specific reference was made to contributions to the system strength by the claddings.

4.2 Top Plate Model

Reardon and Xu (1993) showed that the nails between the sheathing and the top plate had a greater effect on the stiffness of the plate than the composite action of a pair of top plate members. Therefore, a simple analytical model of a top plate was formulated for the present study to predict the stiffness of the top plate due to composite action between the top plate and sheet materials attached to it. This section describes the formulation of the model and presents some sample load-deflection responses. The remainder of the load-deflection responses generated by the model are presented alongside the experimental measurements in Section 4.4.

The top plate model was developed within a Microsoft Excel (Microsoft, 1992) spreadsheet. Classical beam theory was used to calculate the deflection at a number of selected load points along the length of the top plate. The components of the model are illustrated in Figure 15. Superposition was used to calculate the elastic deflection at each load point along the top plate. The load points included the externally applied load and the nail positions which produced restraining forces as the top plate moved relative to the sheet material. An iterative force balancing process was required for each increment of applied load because the nail forces were a non-linear function of the movement between the top plate and sheet. The internal Excel 'Solver' was used to balance the nail forces by minimising the difference between an initial guess of each nail force and the force calculated using the movement of the top plate at each nail position. The contact friction between composite top plates was ignored. It was assessed as contributing significantly less resistance than the sheathing nails.

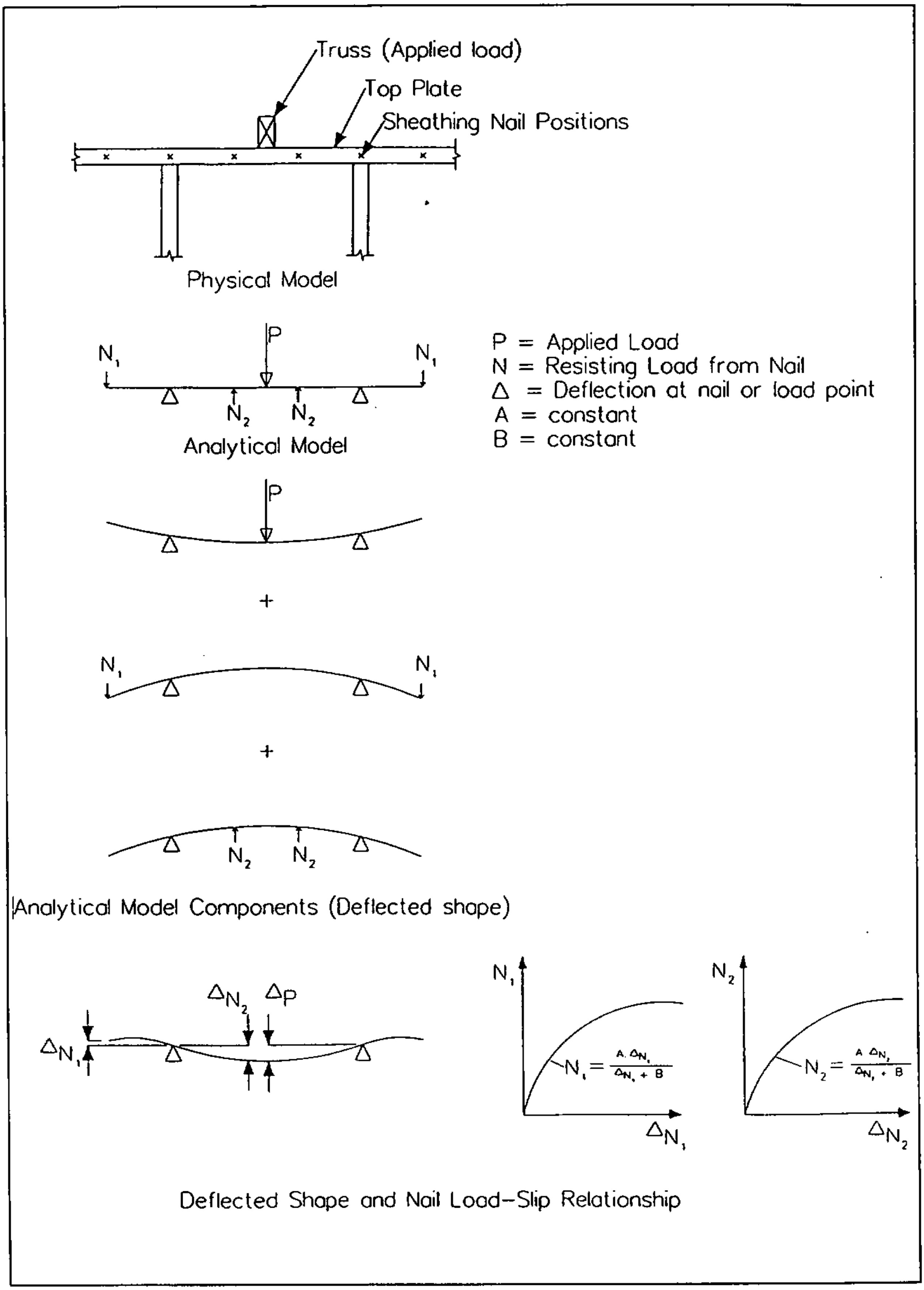

Figure 15. Components of the analytical top plate model.

4.3 Experimental Details

The aim of this investigation was to determine the contribution from common wall sheathing materials to the strength and stiffness of top plates subjected to gravity loads at the midpoint between studs (ie simulation of rafter or truss loads).

4.3.1 Construction Details

Two series of tests were conducted. In the first, two kiln dried 90 x 45 studs were spaced 600mm apart and in the second the spacing was reduced to 400mm. Lining materials used were 9.5mm gypsum plasterboard and 7.5mm fibre-cement sheet. A schedule of the test setups is presented in Table 5. Details of the test specimens are shown in Figure 16.

Table 5 Lining Contribution Tests

Specimen No.	Top plate size (mm x mm)	Stud spacing (mm)	Lining material*
A1	90 x 45	600	Gypsum plasterboard one side
A2	90 x 45	600	Gypsum plasterboard both sides
A3	90 x 45	600	Fibre-cement sheet one side
A4	90 x 45	600	Fibre-cement sheet one side, gypsum plasterboard one side
B1	90 x 45	400	Gypsum plasterboard one side
B2	90 x 45	400	Fibre-cement sheet one side, gypsum plasterboard one side
B3	2 - 90 x 45 nailed together with 2 - 100 x 4.0 nails at 300 centres	400	Gypsum plasterboard one side
B4	2 - 90 x 45 nailed together with 2 - 100 x 4.0 nails at 300 centres	400	Gypsum plasterboard both sides

* Gypsum plasterboard nailed with 30 x 2.5 clouts at 300mm centres
Fibre-cement sheet nailed with 40 x 2.5 flat head nails at 150mm centres

4.3 Experimental Details

The aim of this investigation was to determine the contribution from common wall sheathing materials to the strength and stiffness of top plates subjected to gravity loads at the midpoint between studs (ie simulation of rafter or truss loads).

4.3.1 Construction Details

Two series of tests were conducted. In the first, two kiln dried 90 x 45 studs were spaced 600mm apart and in the second the spacing was reduced to 400mm. Lining materials used were 9.5mm gypsum plasterboard and 7.5mm fibre-cement sheet. A schedule of the test setups is presented in Table 5. Details of the test specimens are shown in Figure 16.

Table 5 Lining Contribution Tests

Specimen No.	Top plate size (mm x mm)	Stud spacing (mm)	Lining material*
A1	90 x 45	600	Gypsum plasterboard one side
A2	90 x 45	600	Gypsum plasterboard both sides
A3	90 x 45	600	Fibre-cement sheet one side
A4	90 x 45	600	Fibre-cement sheet one side, gypsum plasterboard one side
B1	90 x 45	400	Gypsum plasterboard one side
B2	90 x 45	400	Fibre-cement sheet one side, gypsum plasterboard one side
B3	2 - 90 x 45 nailed together with 2 - 100 x 4.0 nails at 300 centres	400	Gypsum plasterboard one side
B4	2 - 90 x 45 nailed together with 2 - 100 x 4.0 nails at 300 centres	400	Gypsum plasterboard both sides

* Gypsum plasterboard nailed with 30 x 2.5 clouts at 300mm centres
Fibre-cement sheet nailed with 40 x 2.5 flat head nails at 150mm centres

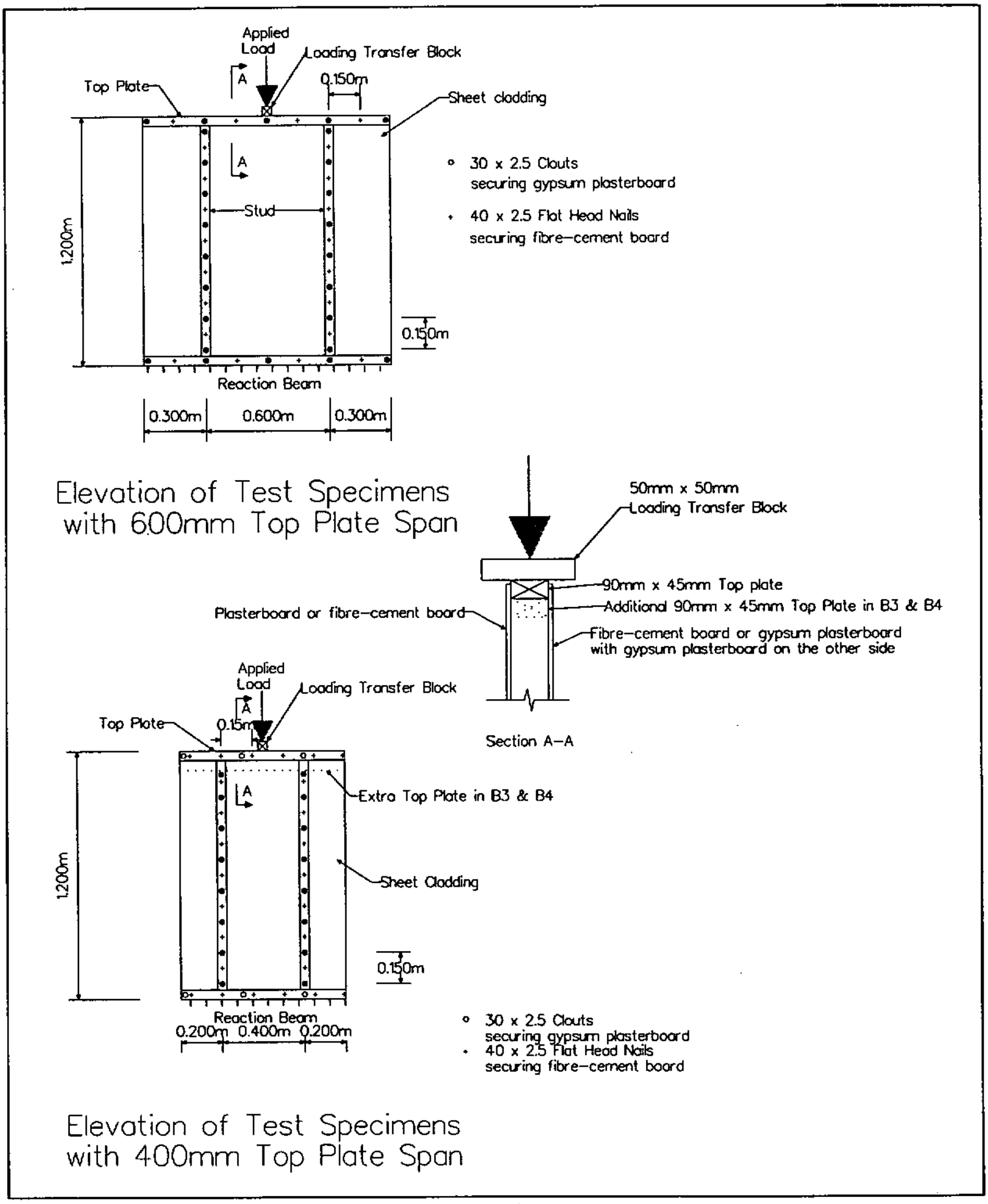

Figure 16. **Details of Investigation 3 test specimens.**

4.3.2 Loading

Top plate members were loaded at a rate of approximately 1 kN/minute to a maximum load of 6 kN initially, to ascertain their bending stiffness with no lining materials attached. The linings were then installed and load was again applied to the top plate at the same loading rate. In both cases the load was applied through a 45mm wide timber block simulating the bottom chord of a truss or a rafter.

4.3.3 Instrumentation

The applied load was monitored by a 22 kN loadcell calibrated within BS 1610 Grade 1 (BSI, 1985) accuracy. The loads transferred to the two studs directly from the top plate were monitored with two 10 kN calibrated loadcells recessed into the tops of the studs. Deflection of the top plate was monitored with a linear potentiometer at midspan between the studs. Potentiometers were also used to monitor the slip between the studs and the sheathing and the total vertical displacement of the sheathing. Because the slippage was minimal between the studs and the sheathing, the vertical sheathing displacement was subtracted from the top plate midspan deflection to determine the deflection of the plate with respect to the top of the studs.

4.4 Results

Plots of applied load, load carried directly to the studs by the top plates and load transferred to the studs via the sheathing material for the eight specimens tested are presented in Figure 17 to Figure 24. It can be seen from Figure 17, Figure 18 and Figure 21 that only a small proportion of the applied load is transferred to the studs via the sheathing in the case of the walls lined with gypsum plasterboard only. As expected, the proportion carried by the sheathing is approximately doubled when a second sheet of gypsum plasterboard is added (cf Figure 17 and Figure 18). A fibre-cement sheathing was found to transfer a much greater proportion of the load to the studs than gypsum plasterboard because of the stiffer connection at the nails and the greater internal stiffness of the sheet (Figure 19). When the deflections are less than 0.5 mm the sheathing actually transfers more than 50% of the applied load. However, as the deflection increases beyond this value a greater proportion is transferred directly to the studs by the top plate as the nailed connections degrade.

A comparison between the recorded centre span deflection of the top plate for each specimen and the predicted deflection from the Excel spreadsheet model was made. The results of this comparison are plotted in Figure 25 to Figure 32. The model predicts the deflection of the top plate alone using simple beam theory and this is compared with the experimental results for the top plates used in the specimens. The model then takes account of the strength and stiffness of the nails fixing the sheathings to the timber frame. Adjustment of the elastic modulus of the top plate timber, the strength of the sheathing nails and the quasi-stiffness of the sheathing nails can be made within the model. Experimentally determined values for these parameters were inserted (eg elastic modulus) or estimated from previous work (Thurston, 1995) and the experimental load deflection plots for both the unsheathed and the sheathed specimens were compared with the analytically predicted curves. Quite reasonable agreement was able to be achieved between the predicted and the experimental deflections for the unsheathed frames, provided a constant displacement offset was included. The initial steepening of the curve was thought to be due to local crushing of the top plate where it bore on the top of the studs. This contribution to the stiffness of the plate is not taken into account in the simple beam theory prediction of the deflection. Therefore, a zero load offset was included once the match to the slope of the straight portion of the line had been achieved.

The associated prediction for sheathed specimens was generally not so well matched. In these cases there was no local crushing of the top plate because this had already occurred when the plate was loaded with no sheathings attached.

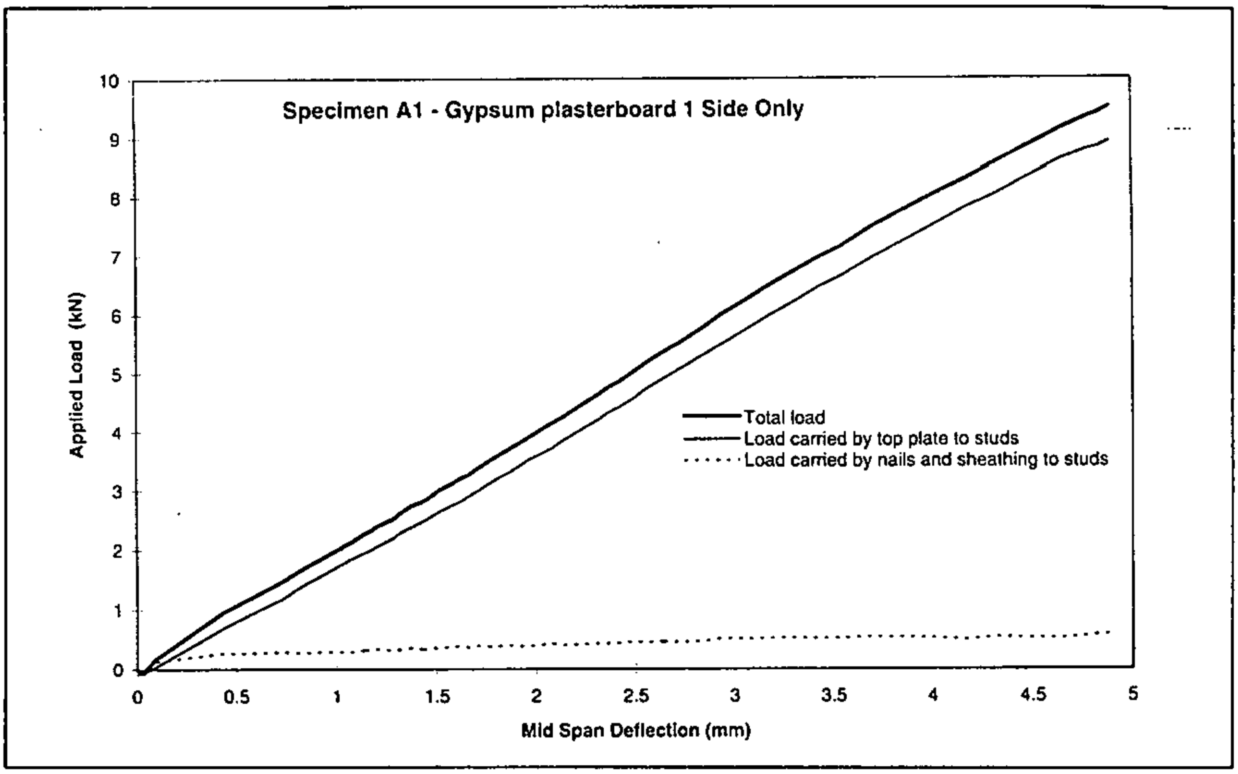

Figure 17 Deflection contributions for Specimen A1.

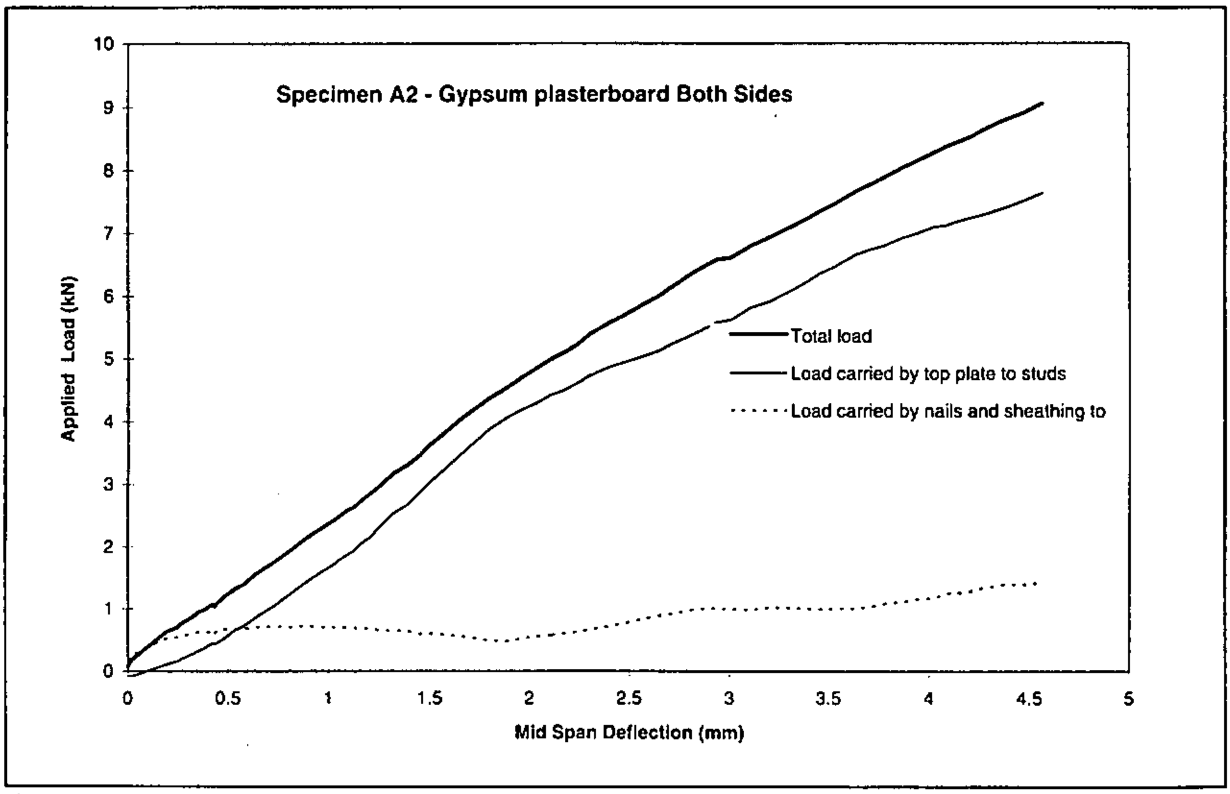

Figure 18 Deflection contributions for Specimen A2.

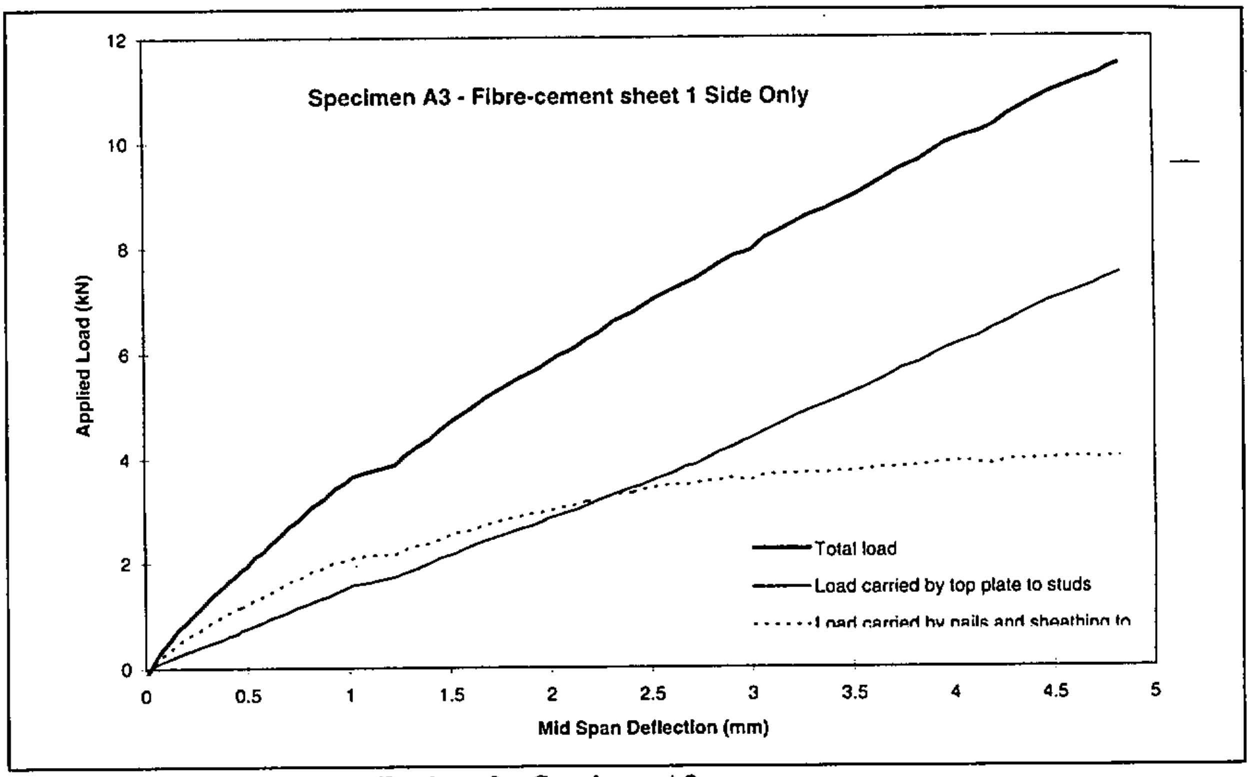

Figure 19 Deflection contributions for Specimen A3.

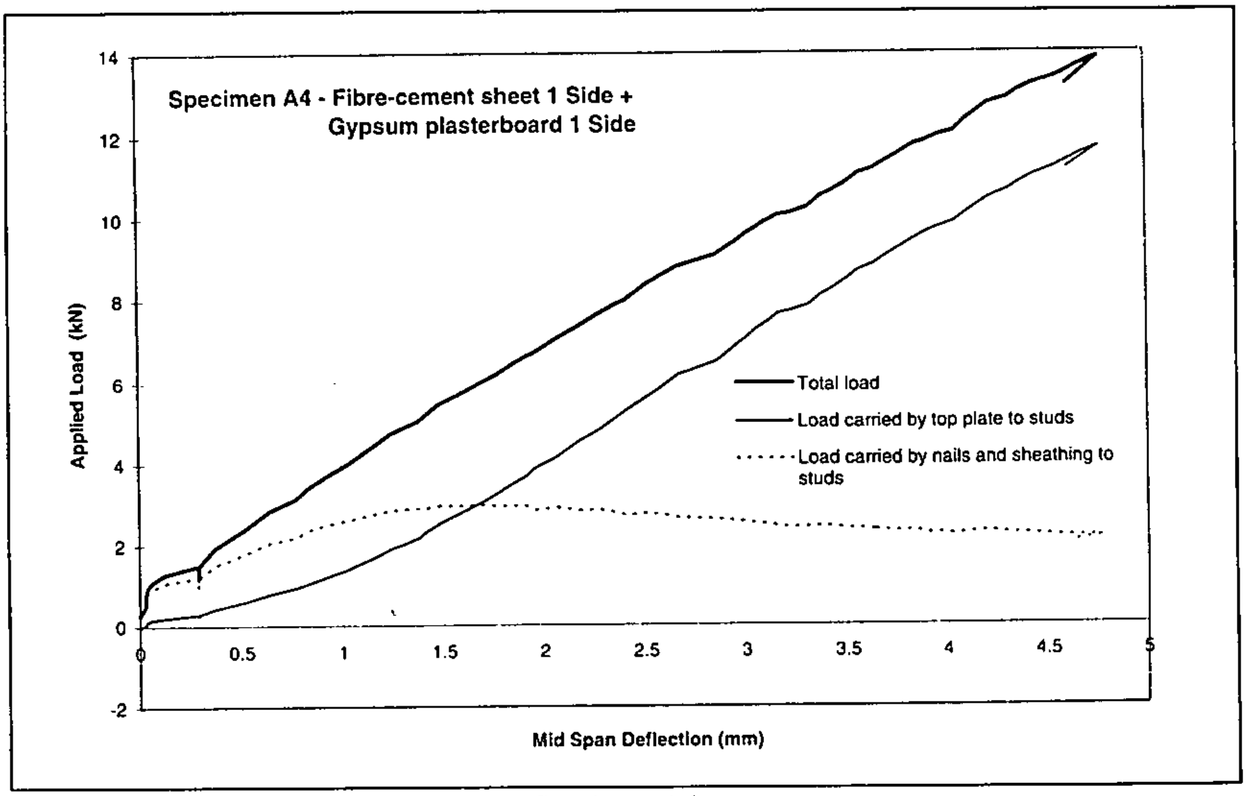

Figure 20 Deflection contributions for Specimen A4.

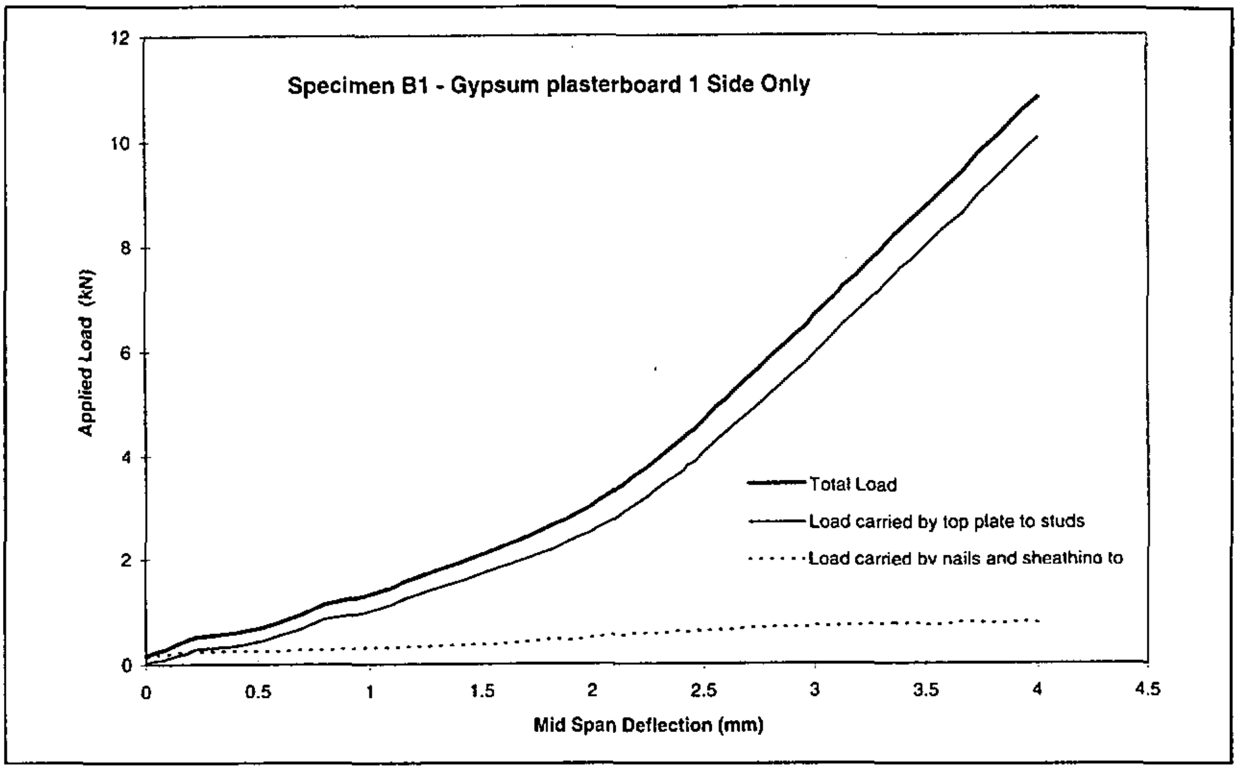

Figure 21 Deflection contributions for Specimen B1.

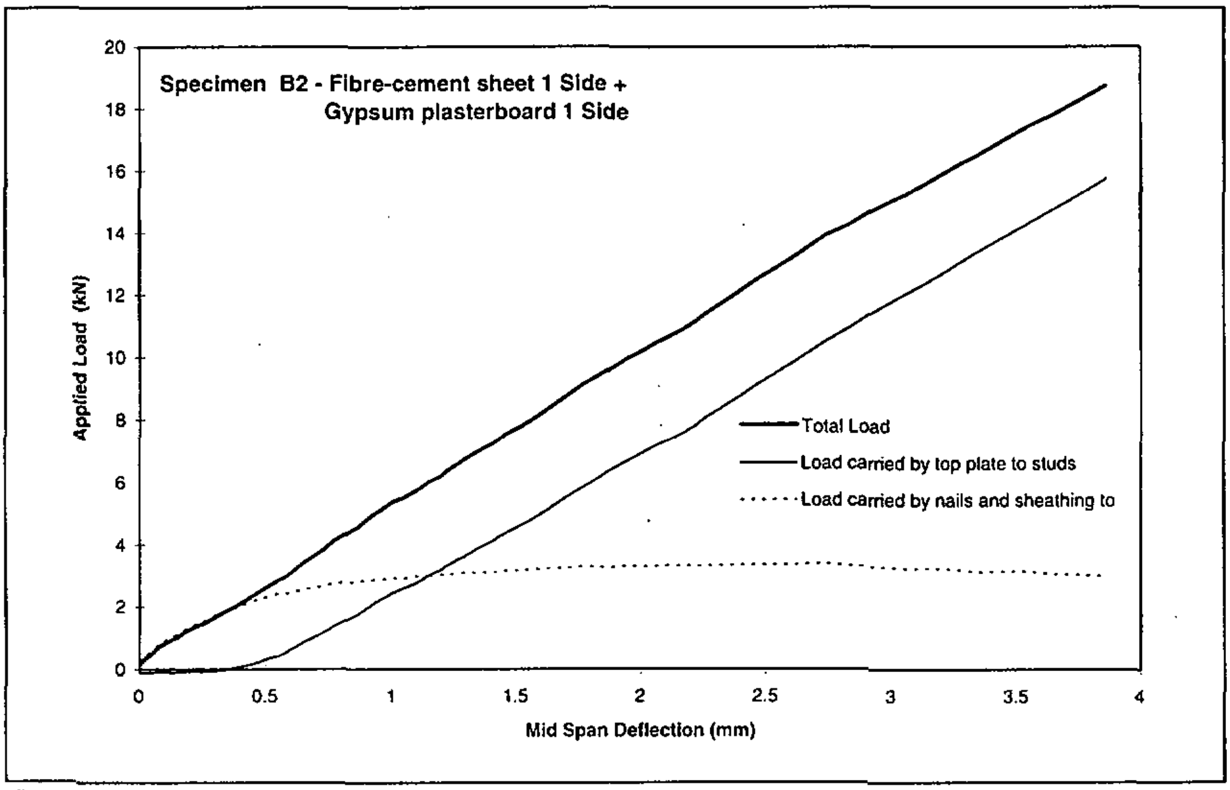

Figure 22 Deflection contributions for Specimen B2.

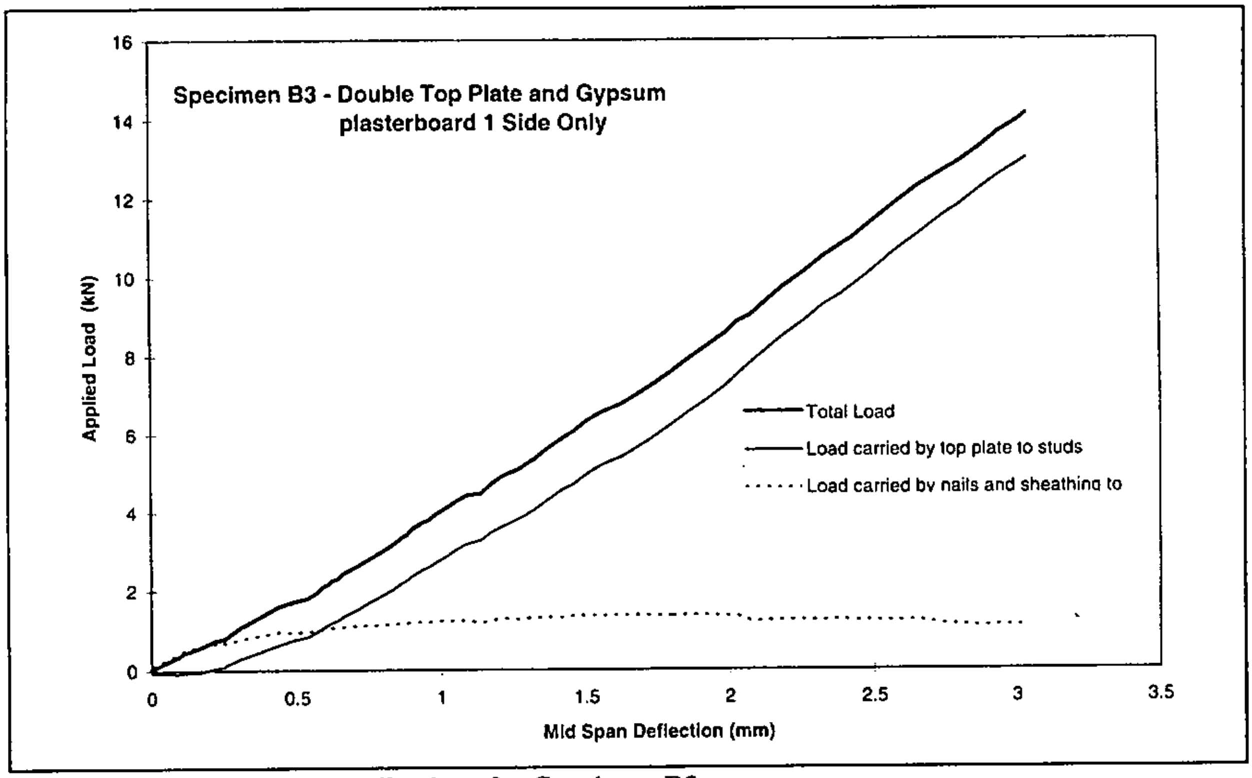

Figure 23 Deflection contributions for Specimen B3.

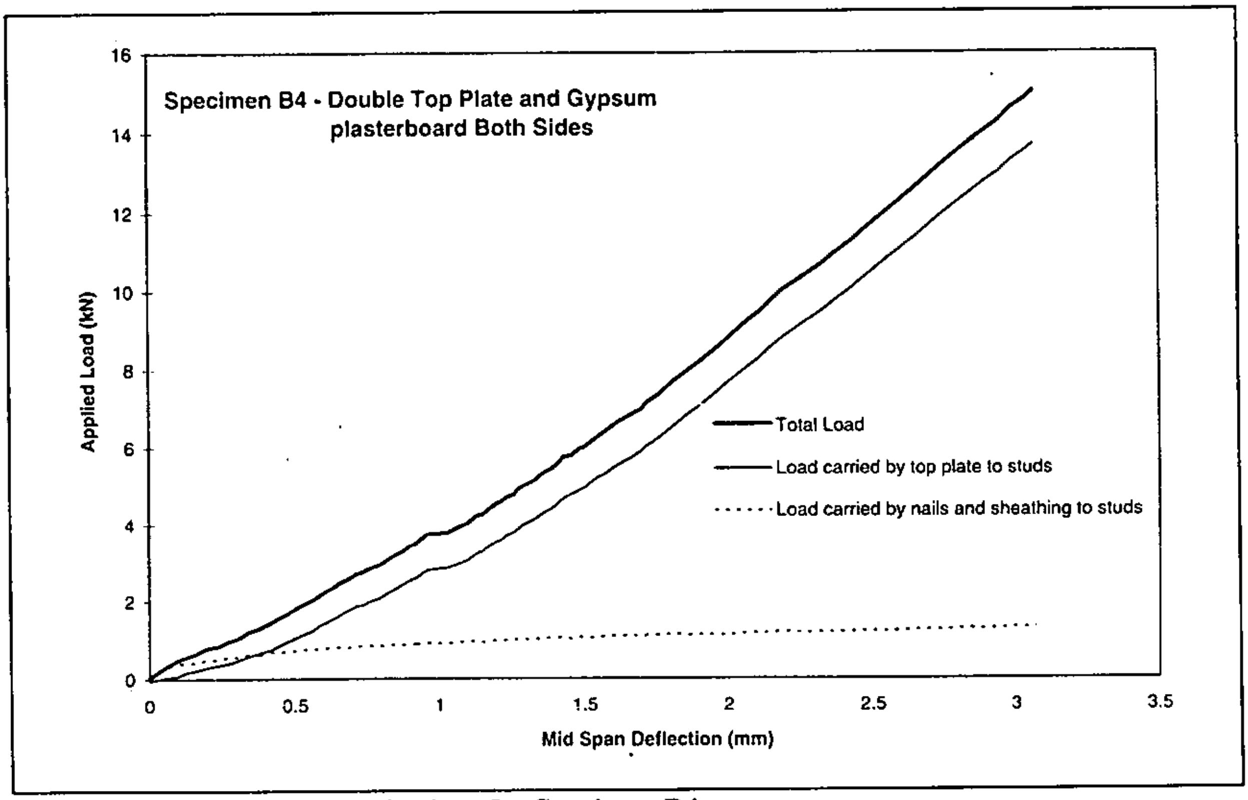

Figure 24 Deflection contributions for Specimen B4.

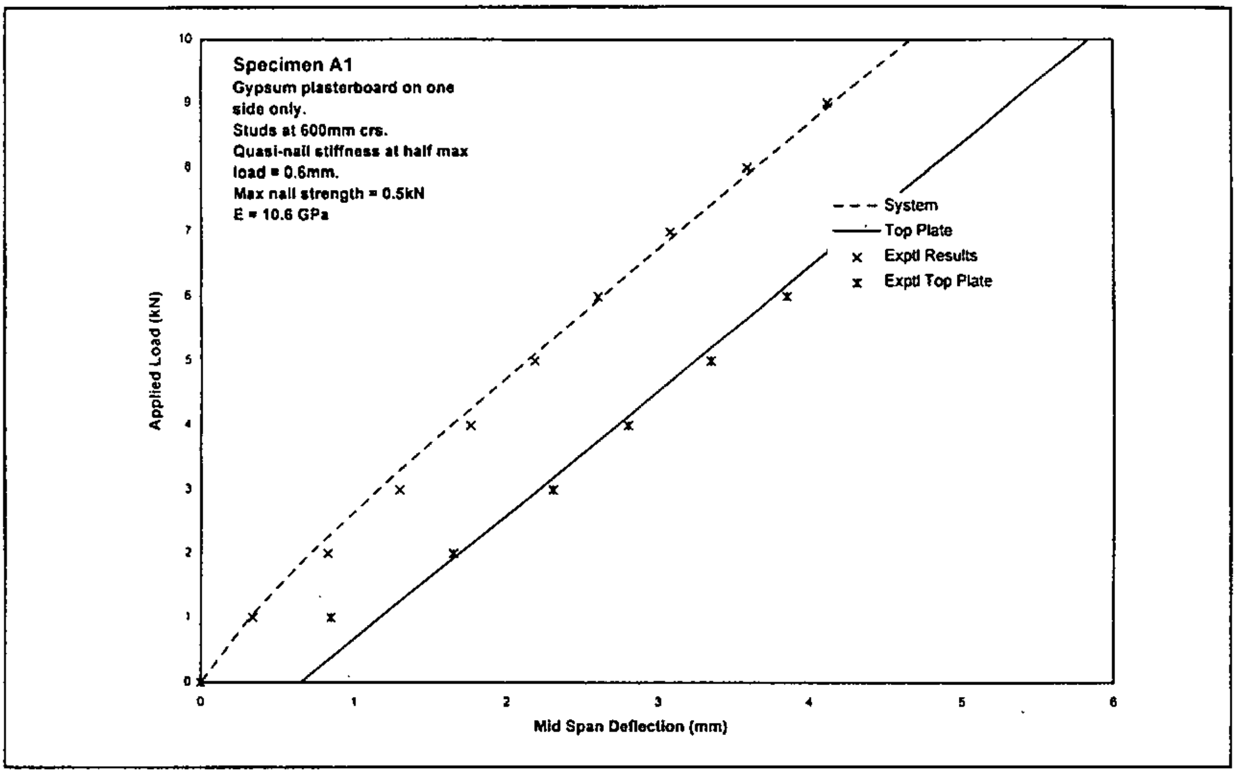

Figure 25 Comparison of experimental stiffness and model prediction - Specimen A1.

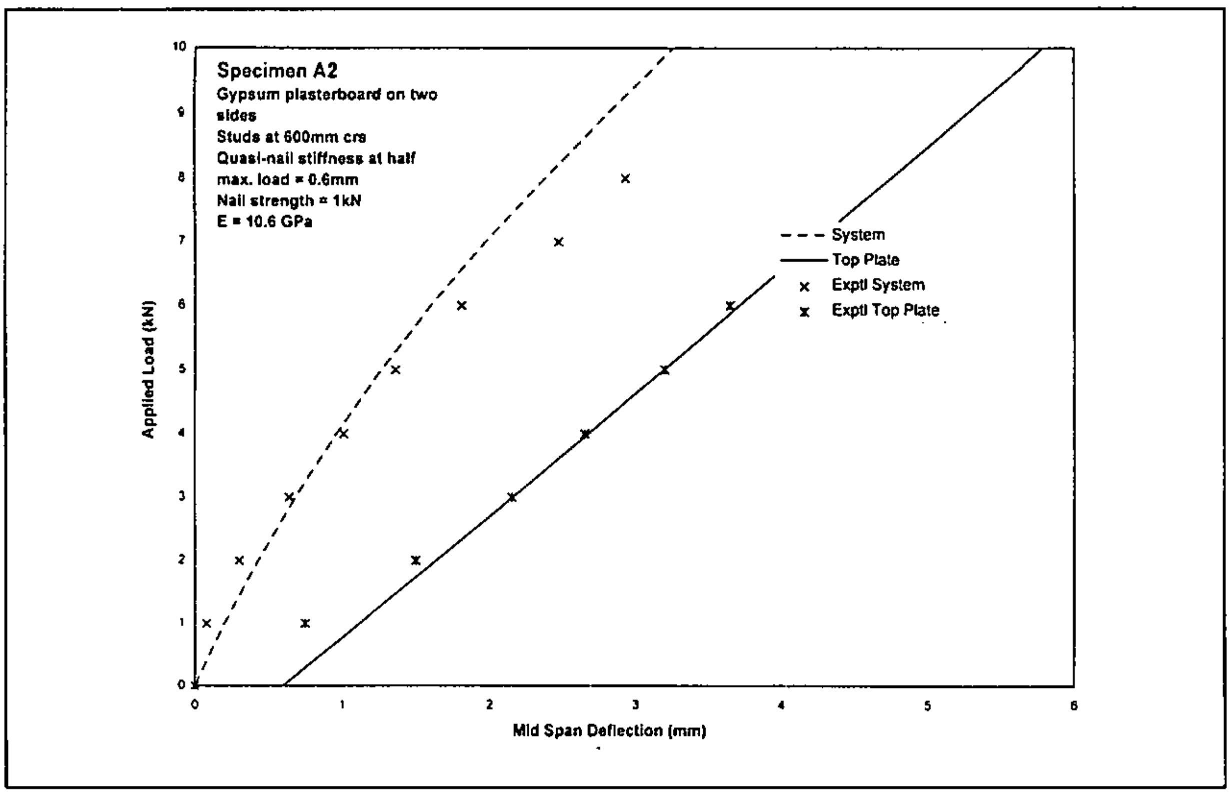

Figure 26 Comparison of experimental stiffness and model prediction - Specimen A2.

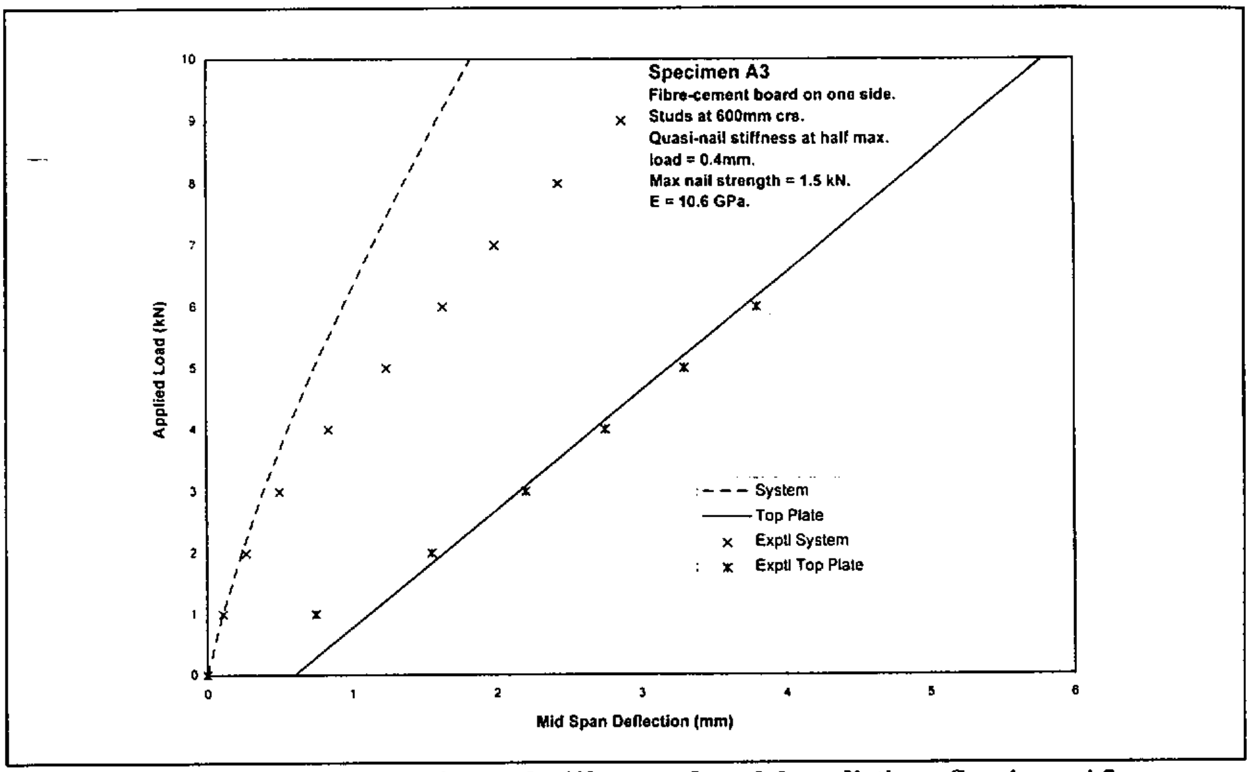

Figure 27 Comparison of experimental stiffness and model prediction - Specimen A3.

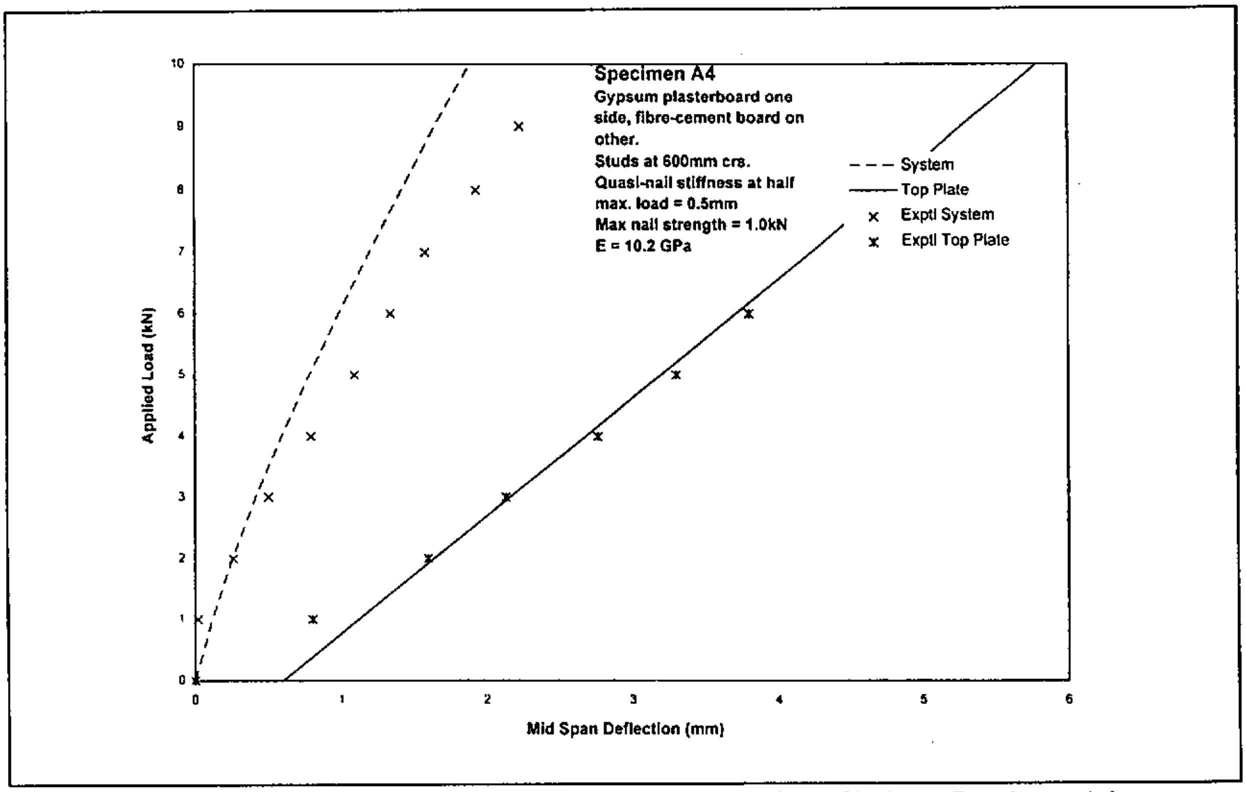

Figure 28 Comparison of experimental stiffness and model prediction - Specimen A4.

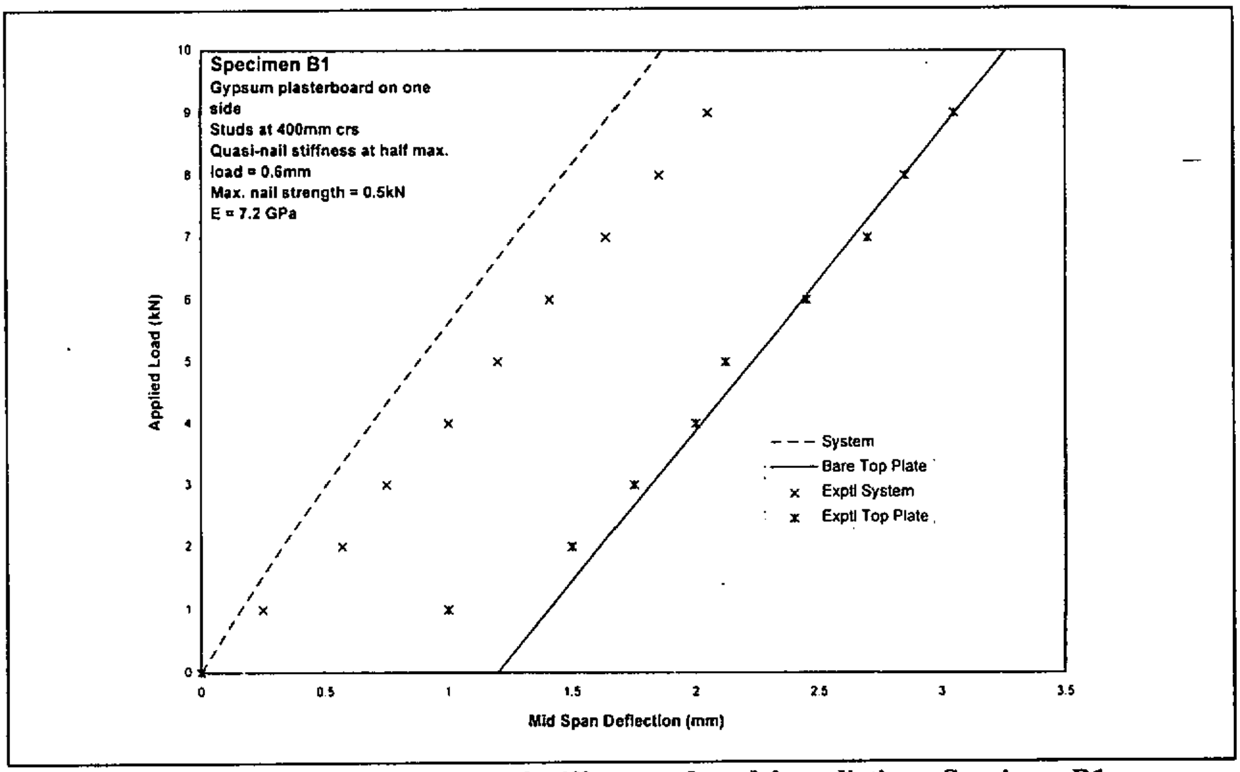

Figure 29 Comparison of experimental stiffness and model prediction - Specimen B1.

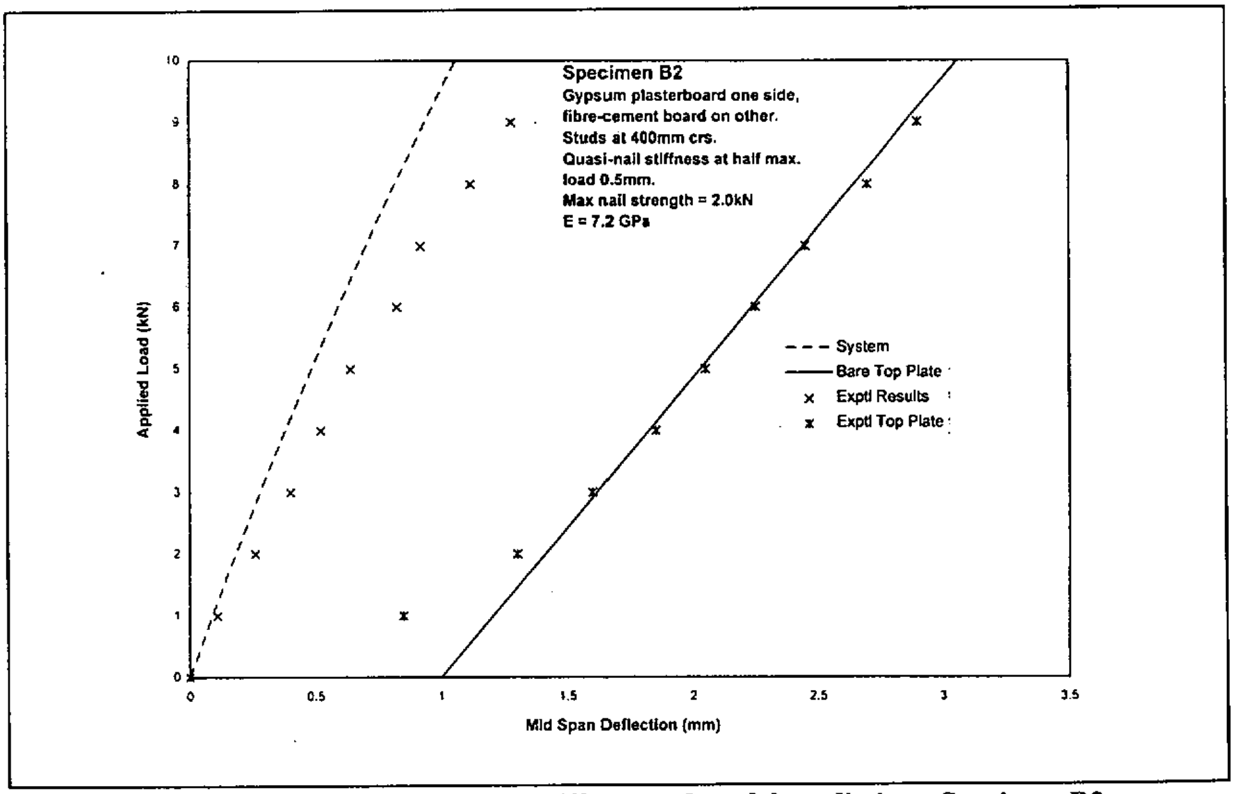

Figure 30 Comparison of experimental stiffness and model prediction - Specimen B2.

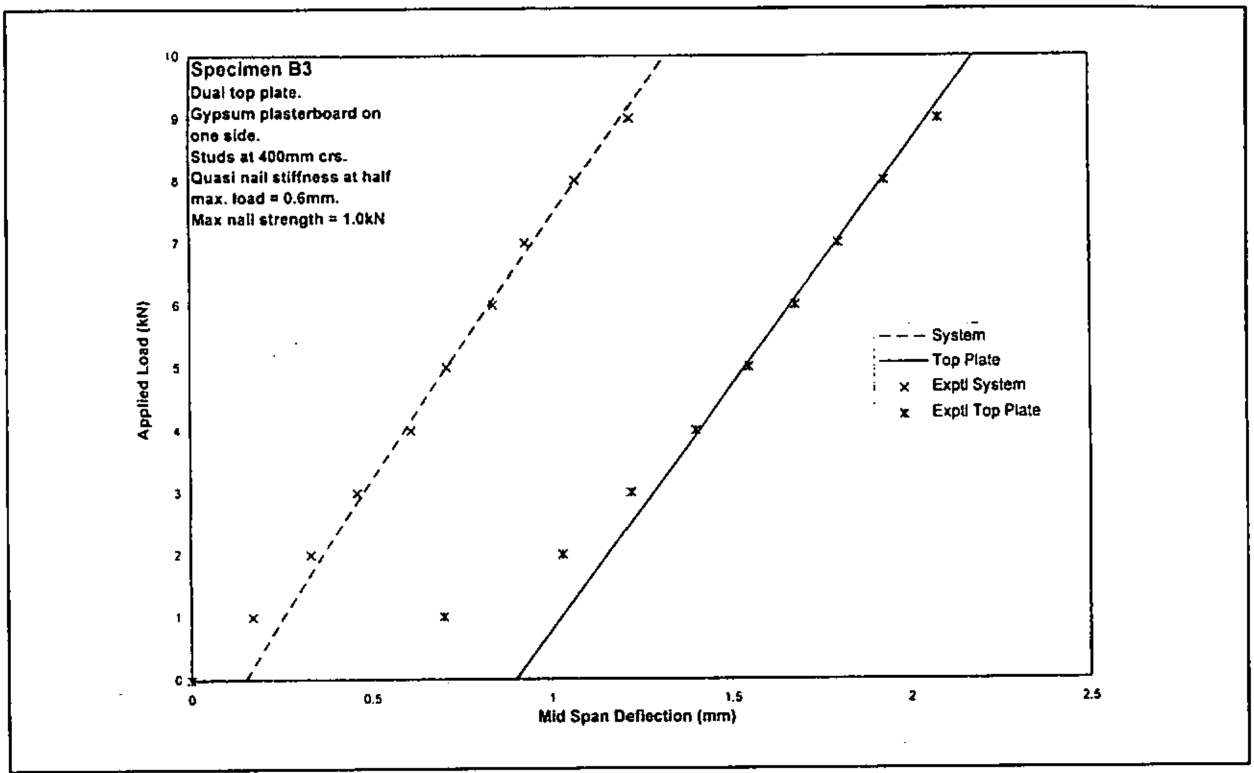

Figure 31 Comparison of experimental stiffness and model prediction - Specimen B3.

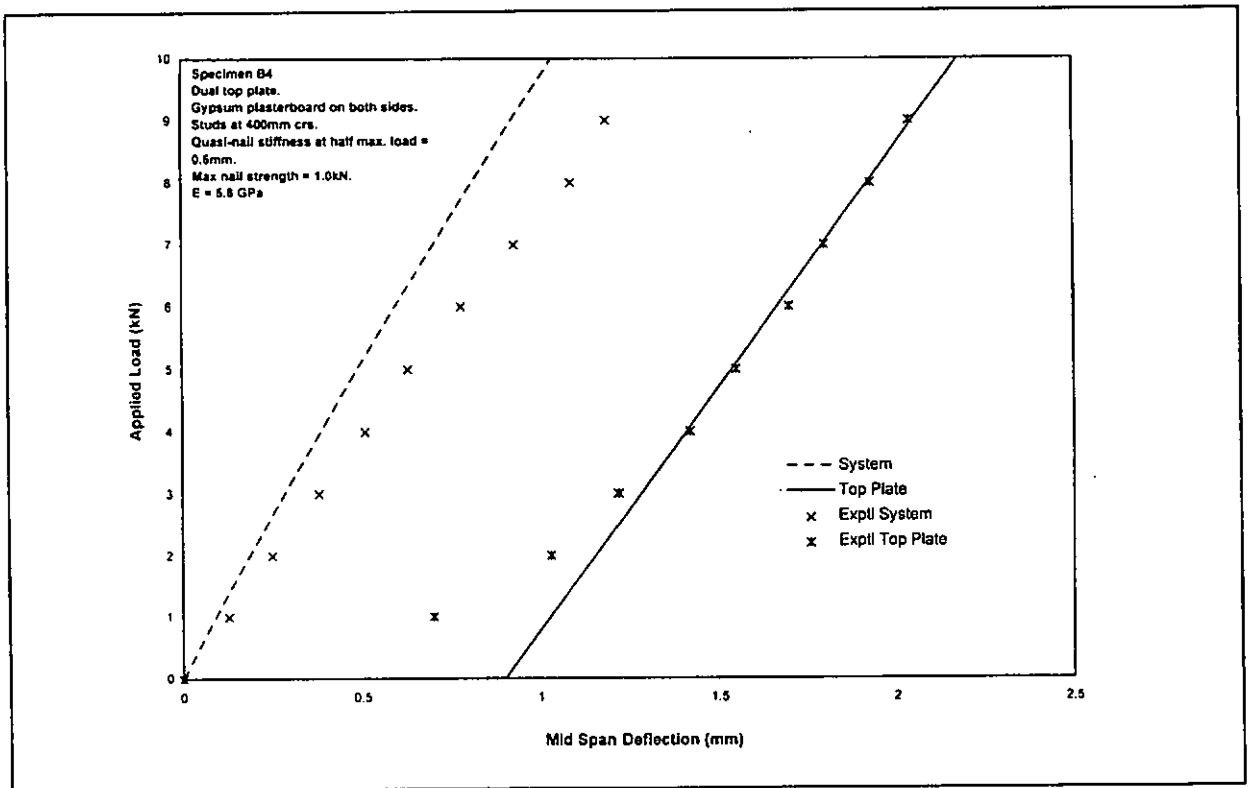

Figure 32 Comparison of experimental stiffness and model prediction - Specimen B4.

5. Conclusions and Recommendations

5.1 Investigation 1 - Composite Behaviour of Face and Axially Loaded Walls

The applied axial load and face loads in the experimental work covered the range of loads expected to be experienced with typical domestic construction under serviceability conditions.

Comparison of the analytical model and the experimental results showed that the service stiffness of the wall system with 9.5mm gypsum plasterboard sheathing nail fixed with pairs of 30 mm × 2.5 mm clouts at 300 mm centres was 1.6 to 2 times the stiffness of a single 2.4 m long 90 mm × 35 mm stud when the sheathing material was in compression. Over the serviceability range of deflections, the behaviour of the composite system when the sheathing is in tension is the same as when it is in compression. The variability of the stiffnesses between the specimens is a reflection of the variability in the material properties of the studs and the connection between the sheathing and the stud.

In view of the small number of specimens, it is suggested that the lower figure of 1.6 be used in the analytical model to estimate serviceability deflections of 90 × 35 mm studs lined with plasterboard. The sensitivity of the mid-span deflection to variations in centroid offset, knot eccentricity and MOE needs to be considered when the model is used to generate stud design tables.

The stiffness of the system with both 7.5mm fibre-cement sheet on one face and 9.5mm gypsum plasterboard on the other was between 2.5 and 4 times the single stud stiffness, depending upon the axial loads applied to the specimen. The analytical model was shown to accurately predict mid-height deflections of the experimentally tested studs and wall systems which were subjected to combined axial and face loads.

Again, it is suggested that the lower end of the range be used in design to estimate the serviceability deflections.

Extension of the model to include heavier sheathing materials and different fixing methods (eg glue, screws and combinations) on similar-sized timber studs will be a straightforward process. It will be necessary to obtain maximum strengths and quasi-nail stiffnesses for the different fixing elements and combinations so that they can be included in the model. The composite action of larger studs with similar sheathing materials will be less pronounced than in this investigation because the stiffness of the stud alone will be a greater proportion of the combined stiffness. Application of the model to the larger studs would therefore not be possible without modification.

The model would require modifications to predict deflections for alternative (steel) frame systems because the joint details between the studs and the top plate ("rails") and the behaviour of the sheathing fasteners will both be different.

5.2 Investigation 2 - Rafter/Top Plate/Stud Connections

The work carried out clearly showed that the strength of the joint between the rafter or truss and the top plate was less than required to resist the expected uplift loads calculated in accordance with NZS 4203 (SNZ,1992) in all but a few cases where the contributing roof area was small or the wind exposure was low. While there has generally been little evidence of failures in the field, suggesting that the existing fixings are satisfactory, extreme events such as those reported by Cooney (1980) and Lim (1990) indicated that uplift loads do exceed the capacity of the fixings.

The effect of sheathing materials, such as gypsum plasterboard on the interior and fibre-cement board on the exterior, on the uplift resistance of the stud to top plate joint was not investigated in this study. Gypsum plasterboard on the inside face of the studs is not expected to provide significant beneficial influence because the wire dogs are positioned on the outer face of the top plate. Under uplift load, the top plate would therefore be expected to rotate about its long axis because of the eccentric load path, leading to premature failure.

It is recommended that in view of the non-conservative test results obtained, further testing be undertaken to establish the strength and stiffness of combinations of nailed and wire dogged truss and rafter connections to top plates which have lining materials in place. It may be necessary to upgrade the connection requirements given in NZS 3604 (SNZ, 1990).

Of further concern was the tendency of the plate and the studs to split when the wire dogs were installed, which appeared to significantly reduce the joint strength. This type of effect will be more common with the use of kiln dried machine stress-graded timber than with visually graded timber because the drier stress-graded timber is more susceptible to splitting and it is thinner. Further investigation of the potential splitting problem is also recommended.

5.3 Investigation 3 - Top Plate Strength Enhancement From Sheathings

The experiments carried out have shown that wall sheathings do have a beneficial influence on the weak axis bending load-resisting capability of top plates. The influence is variable, both with respect to the level of deflection and the type of sheathing material in place, and cannot therefore be modelled either in terms of a constant percentage of the total load or as a constant load.

A composite model which utilised the measured modulus of elasticity of the top plate and the previously determined strength and stiffness parameters for the sheathing nails was found to provide a poor estimation of the behaviour of the system. For all specimens, the model predicted a greater stiffness than was actually achieved experimentally.

In the model, the span of the top plate was taken as the clear distance between the studs, assuming that the pivot point for the deflected plate was at the edge of the stud. While not measured in the experimental work, it is expected that the outer fibres of the plate would crush locally under the concentrated load, resulting in an increase in the effective top plate span. A change to the plate span length in the model, from clear distance between studs to centre to centre distance of the studs, resulted in a significantly reduced analytical stiffness. However, this could be considered as an absolute lower bound on the stiffness because the crushing of the plate would never be likely to extend to the centre width of the stud. More likely, the crushing would extend only about 5 mm onto the stud.

NZS 3604 (SNZ, 1990) requires top plates to be supported by the addition of a 100 x 50 dwang on edge beneath the plate in certain circumstances where the truss or rafter lands beyond 150mm from the centreline of the nearest stud. The results of this investigation indicate that it may be possible to reduce the extent of application of this requirement. Further testing of the supported plate will be necessary to make a direct comparison between the behaviour of a lined and unsupported plate and a supported plate.

6. References

Amana, E.J. and Booth, L.G. 1967. Theoretical and experimental studies on nailed and glued plywood *stressed-skin components: Part I. Theoretical study.* Journal of the Institute of Wood Science. 4(1) 43-69.

British Standards Institution. 1985. Materials testing machines and force verification equipment. Part 1. *Specification for the grading of the forces applied by materials testing machines.* BS1610. London.

Buchanan, A. H. 1986. Combined bending and axial loading in lumber. ASCE Journal of Structural Engineering. 112(12).

Collins, M. J. 1980. The engineering bases for the plate tables in NZS 3604 code of practice for light timber frame buildings. New Zealand Forest Service, Forest Research Institute, Forest Products Division Report No FP/TE 35. (unpublished)

Cooney, R.C. 1980. The Te Aroha storm of 19 July 1978 - damage to buildings. Building Research Association of New Zealand Technical Paper P29. Judgeford.

Deam, B.L. 1993. A *design procedure for timber stud wall framing.* Part 1: End fixity and lining contributions. (Unpublished confidential). Building Technology Limited Report STR 5100/1.

Deam, B.L. and King, A.B. 1994. Research Supporting AS 1684 Framing Code Revision. *Proceedings, Pacific Timber Engineering Conference,* Gold Coast, Australia, 11-15 July, 1994. 1:131-139.

Gromala, D.S. and Polensek, A. 1983. Analysis and design of wall systems under axial and bending loads. *Proceedings, FPRS 7317 Wall and Floor Systems: Design and Performance of Light-frame structures,* Denver, Colorado. 87-100.

Gromola, D.S. and Polensek, A. 1984. Light-frame wall research - Axial and bending loads, Housing *Science, 8(4):* 383-393.

Lim, K.Y.S. 1990. Tornado Damage at Inglewood. Miscellaneous report. Building Research Association of New Zealand. Judgeford.

Microsoft Corporation. 1992. Microsoft® Windows™ Excel 5.0.

Polensek, A. 1976. Finite element analysis of wood stud walls. Journal of the Structural Division, ASCE, 102(ST7): 1317-1335.

Polensek, A. and Atherton, G.H. 1976. Compression-bending strength and stiffness of walls with utility grade studs. Forest Products Journal, 26(11): 17-25.

Polensek, A. and Schimel, B.D. 1986. Rotational restraint of wood-stud wall supports. Journal of Structural Engineering, ASCE, 112(6): 1247-1262.

Reardon, G. and Xu, Y.L. 1993, Multiple top plates (Ribbon plates), (Unpublished) Department of Civil and Systems Engineering Report, James Cook University, Townsville, Queensland.

Sherwood, G. and Moody, R.C. 1989. Light-frame wall and floor systems: Analysis and performance, Forest Products Lab. Report FPL-GTR-59,23-33.

Standards Association of New Zealand. 1978. Code of practice for light timber frame buildings not requiring specific design. NZS 3604. Wellington.

Standards Association of New Zealand. 1990. Code of practice for light timber frame buildings not requiring specific design. NZS 3604. Wellington.

Standards New Zealand. 1992a. Code of practice for general structural design and design loadings for buildings. NZS 4203. Wellington.

Standards New Zealand. 1992b. Timber - stress graded - In-grade strength and stiffness evaluation. AS/NZS 4063. Wellington.

Standards New Zealand. 1992c. Builder's Guide to NZS 3604. MP3600:Part 1. Wellington.

Standards New Zealand. 1993. Timber structures standard. NZS 3603. Wellington.

Thurston, S.J. 1995. Report on racking resistance of long sheathed timber framed walls with openings. Building Research Association of New Zealand Study Report No 54. Judgeford.

Appendix A Expected Loads for Phase 2 Connections

Contributing Roof Areas

NZS 3604 (SNZ, 1990) provides limits on the the use of skewed nails alone between rafters and top plates and end nails alone between top plates and studs. These limits are repeated below for reference:

Rafter fixing requirements are specified as follows:

Rafter or jack rafter to top plate (a) Light roof in very high wind exposure when: (i) the rafter span exceeds 2.5m, or (ii) the rafter spacing exceeds 900mm	2 skewed 100 x 3.75 nails plus cyclone tie with capacity of 16kN
(b) Light roof in high wind exposure when: (i) the rafter span exceeds 2.5m, or (ii) the rafter spacing exceeds 900mm	2 skewed 100 x 3.75 nails plus 2 wire dogs
(c) Light roof in medium wind exposure when: (i) the rafter span exceeds 5m, or (ii) the rafter spacing exceeds 900mm and the rafter span exceeds 3m	2 skewed 100 x 3.75 nails plus 2 wire dogs
(d) Light roof in low wind exposure when: (i) the rafter spacing exceeds 900mm and the rafter span exceeds 4.5m	2 skewed 100 x 3.75 nails plus 2 wire dogs
(e) All other cases	2 skewed 100 x 3.75 nails

From the above limitations and using Table 10.2 from NZS 3604 (SNZ, 1990), for framed roofs the **maximum** contributing areas to rafter/plate connections are:

Light roof in low wind exposure	$(6.2/2 + 0.75) \times 1.2 = \mathbf{4.62m^2}$
Light roof in medium wind exposure	$(6.2/2 + 0.75) \times 1.2 = \mathbf{4.62m^2}$ or $(6.8/2 + 0.75) \times 0.9 = \mathbf{3.74m^2}$
Light roof in high wind exposure	$(6.2/2 + 0.75) \times 1.2 = \mathbf{4.62m^2}$

In all of the above cases NZS3604 (SNZ, 1990) requires 2 skewed 100 x 3.75 nails plus two wire dogs. Maximum contributing areas for 2 skewed 100 x 3.75 nails only have been calculated from the above table as follows:

Light roof in low wind exposure	$(4.5/2 + 0.75) \times 0.9 = \mathbf{2.7\ m^2}$
Light roof in medium wind exposure	$(5.0/2 + 0.75) \times 1.2 = \mathbf{3.9m^2}$ or $(3.0/2 + 0.75) \times 0.9 = \mathbf{2.0m^2}$
Light roof in high wind exposure	$(2.5/2 + 0.75) \times 1.2 = \mathbf{2.4m^2}$ or $(6.8/2 + 0.75) \times 0.9 = \mathbf{3.74m^2}$

A minimum truss fixing to a top plate is 2-100mm skewed nails plus 2 wire dogs or a 5kN capacity fixing. In high wind areas an additional fixing of pairs of 4.9mm wire dogs or an alternative fixing of 5kN capacity is required between the top plate and the supporting wall members at spacings of not more than 900mm if the truss clear span exceeds 7.2m.

The maximum allowable roof area contributing load to a truss to plate connection is:

(Half maximum truss span + eaves overhang) x Maximum truss spacing
= (12/2 + .75) x 1.2 = **8.1m²**

Wind Loads

The four categories of Design Wind Speed and associated Wind Pressure in NZS3604 (SNZ, 1990) are as follows:

Wind exposure	Design Wind Speed (m/s)	Design Wind Pressure (Pa)
Low	32	614
Medium	37	821
High	44	1162
Very High	50	1500

For anything other than a rare occasion the combination of the external and internal pressure coefficients gives a multiplier of 1.1 on the design wind pressures. For the ultimate design load combination of 0.9G & W_u (see NZS 4203 (SNZ, 1992a)), the following uplift loads may be expected on the truss/plate and rafter/plate joint requiring **2 skew nails and 2 wire dogs**:

Truss in very high wind exposure (0.9 x 0.25 - 1.1 x 1.5) x 8.1 = **-11.54 kN**

Framed light roof in high wind exposure (0.9 x 0.28 - 1.1 x 1.162) x 4.62 = **-4.74 kN**

Framed light roof in medium wind exposure (0.9 x 0.28 - 1.1 x 0.821) x 4.62 = **-3.01 kN**

Framed light roof in low wind exposure (0.9 x 0.28 - 1.1 x 0.614) x 4.62 = **-1.96 kN**

For situations with **2 skew nails only** (no wire dogs) the design loads are:

Framed light roof in a high wind exposure (0.9 x 0.28 - 1.1 x 1.162) x 3.74 = **-3.84 kN**

Framed light roof in a medium wind exposure (0.9 x 0.28 - 1.1 x 0.821) x 3.90 = **-2.54 kN**

Framed light roof in a low wind exposure (0.9 x 0.28 - 1.1 x 0.614) x 2.70 = **-1.14 kN**

Appendix B Proprietary Products Used in the Research

Two proprietary sheathings were used in the experimental programme described in this report.

The gypsum plasterboard was nominal 9.5mm standard Gib® plasterboard supplied by Winstone Wallboards Limited.

The fibre-cement board was 7.5mm Harditex™ supplied by James Hardie Building Products Limited.

Note: ***Results obtained in this study relate only to the samples tested, and not to any other item of the same or similar description. BRANZ does not necessarily test all brands or all types available within the class of items tested, and exclusion of any brand or type is not to be taken as any reflection on it.***

This work was carried out for specific research purposes, and BRANZ may not have assessed all aspects of the products named which would be relevant in any specific use. For this reason, BRANZ disclaims all liability for any loss or other deficit, following use of the named products, which is claimed to be based on reliance on the results published here.

Further, the listing of any trade or brand names above does not represent endorsement of any named product nor imply that it is better or worse than any other available product of its type. A laboratory test may not be exactly representative of the performance of the item in general use.

BRANZ

THE RESOURCE CENTRE FOR BUILDING EXCELLENCE

BRANZ MISSION

To be the leading resource for the development of the building and construction industry.

HEAD OFFICE AND RESEARCH CENTRE

Moonshine Road, Judgeford
Postal Address - Private Bag 50908, Porirua
Telephone - (04) 235-7600, FAX - (04) 235-6070

REGIONAL ADVISORY OFFICES

AUCKLAND
Telephone - (09) 526 4880
FAX - (09) 526 4881
419 Church Street. Penrose
PO Box 112-069, Penrose

WELLINGTON
Telephone - (04) 235-7600
FAX - (04) 235- 6070
Moonshine Road, Judgeford

CHRISTCHURCH
Telephone - (03) 366-3435
FAX (03) 366-8552
GRE Building
79-83 Hereford Street
PO Box 496